THE GOUGING PHENOMENON AT LOW RELATIVE SLIDING VELOCITIES
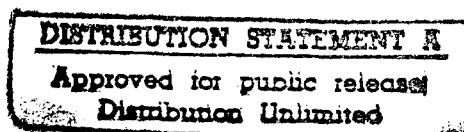
by

KENNETH ROBERT TARCZA, B.S.M.E

THESIS

Presented to the Faculty of the Graduate School of

The University of Texas at Austin

in Partial Fulfillment

of the Requirements

for the Degree of

MASTER OF SCIENCE IN ENGINEERING

The University of Texas at Austin

December, 1995

THE GOUGING PHENOMENON AT LOW RELATIVE SLIDING VELOCITIES

Accesion For	
NTIS CRA&I	☑
DTIC TAB	☐
Unannounced	☐
Justification	
By	
Distribution /	
Availability Codes	
Dist	Avail and / or Special
A-1	

Approved by
Supervising Committee:

William F. Weldon

Richard A. Marshall

Dedication

To the Jews who had believed him, Jesus said, *"If you hold to my teaching you are really my disciples.* **Then** *you will know the truth and the truth will set you free."*

John 8:31,32

This work is dedicated to the Lord Jesus Christ who created all things and makes all things possible, my loving wife Beth, our bundle of joy whose blessed coming is imminent, and my parents.

Acknowledgments

First and foremost, I would like to thank Professor Bill Weldon for his openness, patience, trust, resources, and faith that I could successfully accomplish what I had set out to do, long before I began and even when I didn't exactly know what it was that I was trying to do.

I would next like to thank Dr. Dick Marshall for agreeing to be the second reader on this thesis even though I'm sure he had many other pressing issues to attend to.

I would like to thank the University of Texas Center for Electromechanics (CEM) in general for providing me the access to the facilities, resources, and personnel without which I would have been unable to succeed. Specifically, I would like to thank Murel O'Neal, Charles Thonig, Tri Dao, and Richard Rodriguez for helping me build a world-class .22 caliber pellet gun, Tony Smyrson, for the hole in my catch tank, Bob Polizzi for his help, wisdom, and letting me invade his lab space, Russell Berwick for keeping me supplied, and Elvin Estes for his help on everything, advice on everything, and his friendship. I am also indebted to Dan Gleasing and Jerry McNeal for doing wonders with my pictures, the critical proof of what has been accomplished. Thanks are due as well to Ray Zowarka who shared with me knowledge gained over years of experience with railguns and gouging.

I am also grateful to the University of Texas Institute for Advance Technology (IAT) for providing me access to a great wealth of wisdom and resources. Specifically, I would like to thank Drs. Dick Marshall and Chady Persad for independently entertaining my fledgling thoughts, Dr. Stephen Bless for providing more insight than I could absorb about impact dynamics and access to the IAT library, and Lisa Bradley, the IAT librarian who provided me more references than I could assimilate in a lifetime.

I must also thank Dr. Zwy Eliezer who unknowingly planted the first seed about this project and made seem simple the complexities of friction and wear.

I am indebted to the United States Army for funding this course of study and providing me with unparalleled opportunities to excel.

Most importantly, I must thank my wife Beth for her unending patience, love and support through my strugglings. She is the wind beneath my wings.

Submitted to committee for approval in October, 1995

ABSTRACT

THE GOUGING PHENOMENON AT LOW RELATIVE SLIDING VELOCITIES

Kenneth Robert Tarcza, M.S.E.

The University of Texas at Austin, 1995

Supervisor: William F. Weldon

Surface gouging by metals in high-velocity sliding contact has been observed for more than thirty years in engineering applications involving rocket sleds, two-stage gas guns, and electromagnetic railguns. The onset of gouging is usually observed to occur at sliding velocities in excess of 1000 m/s (3821 ft/s). Previous investigations of the phenomenon have indicated that the gouging onset velocity is proportional to the yield strength and hardness of the materials involved. In this research, data from actual instances of gouging are used to develop a graphical, linear

correlation between gouging onset velocity and yield strength of the sliding material. This correlation is extrapolated into a velocity regime below that in which gouging is usually observed and then serves as the basis for an experiment intended to produce gouges. In the experiment, gouges are produced on lead sheet at sliding velocities as low as 245 m/s (804 ft/s), well below those at which gouging had previously been reported and in a material never before reported to have gouged, confirming the validity of the extrapolation.

TABLE OF CONTENTS

LIST OF TABLES

LIST OF FIGURES

xvi

CHAPTER 1

INTRODUCTION

At hypervelocity, the regime of velocity in which the predominant forces of interaction are inertial, there exist certain contact phenomena that do not occur at lower velocities [1]. One of these is hypervelocity gouging. Gouging is not a new phenomenon, having been observed in rocket sled testing for more than 30 years [2,3]. It can be described as the localized scarring of a stationary surface (guider) resulting from intermittent contact with a high-velocity object (slider) moving over and parallel to its surface [4].

This type of damage has always been considered an operational nuisance as well as unfortunate side effect of high sliding velocities. More recently, it has also been recognized as a problem which demands time consuming maintenance and costly repairs [2]. A single rocket sled run or railgun shot can produce gouging severe enough to require maintenance. Gouges on rocket sled tracks are repaired either by grinding down raised and rough edges or, in extreme cases, by filling the gouges with new material by welding and then grinding [2]. When gouging occurs in railguns, the rails must be honed at a minimum and replaced if the gouging is severe. In either case, gouging is not only inconvenient but is also an obstacle to the development of long life, rapidly repeatable, hypervelocity systems.

The ideal "solution" to the gouging problem will be found when the initiation of gouging and precise location of gouges can be accurately predicted, and when gouging can be universally prevented rather than

avoided. Until such a solution is found, investigation of the gouging phenomena remains incomplete.

The primary purpose of this research is to demonstrate that gouging is possible at velocities lower than those at which it has been previously reported. It is further intended to show that there exists a correlation between gouging and material properties in slider-guider systems which can be used to fairly accurately predict the gouging onset velocity, and that this correlation can be experimentally validated.

1.1 UNDERSTANDING THE PROBLEM

Gouging damage has been produced by rocket sleds generally at velocities above 1.5 km/s (4922 ft/s) [5-7], by two-stage gas gun projectiles at velocities between 3.0 and 5.4 km/s (9,843 and 17,717 ft/s) [8-11] and by railgun projectiles (armatures), largely between 1.5 and 2.5 km/s (4,922 and 8,203 ft/s) with less damage occurring between 1.2 and 6.6 km/s (3,937 and 21,655 ft/s) [12] and one reported instance occurring at 300 m/s (9,984 ft/s) [1]. Gouges usually appear in the shape of a tear drop, with the wider end being on the "downstream" end of the "drop" and characterized by a slightly raised lip, as shown in Figure 1.1.

VIEW FROM ABOVE

LONGITUDINAL PROFILE   rail surface

DIRECTION OF TRAVEL ⟶
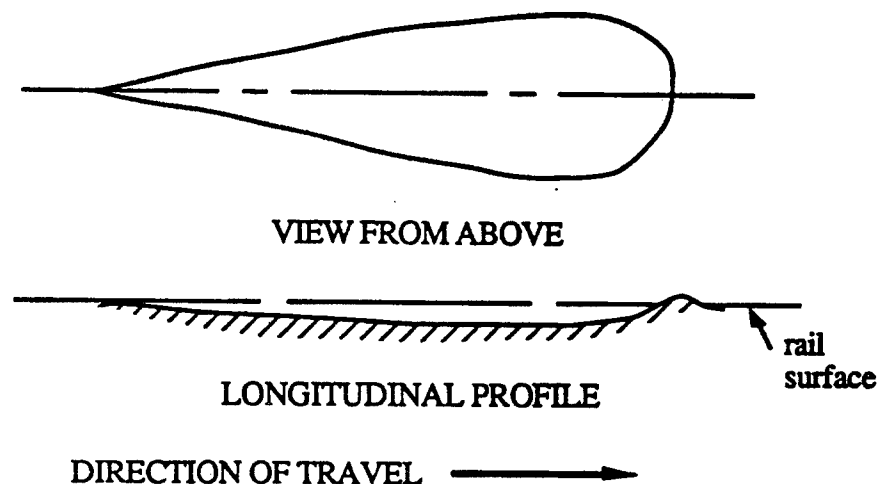
Figure 1.1 - Sketch of a Typical Rail Gouge [2]

The following description of damage that occurred on the rails of a Lawrence Livermore National Laboratories railgun typifies the phenomenon :

A typical gouge in the copper was roughly the shape of a wide, flat-bottomed tear drop, or isosceles triangle, with the apex directed toward the breech and the base toward the muzzle. Rail material was forced forward in the direction of the projectile travel and accumulated in a mound at the base of the triangle. Where small craters occurred, the damage was usually in a cluster of two or three damage sites about 1 to 2 mm across. Larger sites usually occurred near the center of a rail and were typically 3 to 5 mm across the base and from 2 to 5 mm from base to apex. Occasionally, a gouge formed on the interface of the rail and the dielectric, where only the rail was damaged [12].

1.2 UNDERSTANDING THE SYSTEMS INVOLVED

1.2.1 ROCKET SLEDS

Rocket sleds are in fact sleds which are powered by rocket motors but operate at ground level. Similar to concept of a railroad, rocket sleds are guided along a predetermined path of travel by, depending on the sled design, either one or two steel rails. Sled "shoes" on the bottom of a sled assembly attach a rocket sled to it's guiding rail by essentially "gripping" the top portion of the rail(s). Rocket sleds may weigh as much as 18,000 kg

(39,690 lbm) [13] and are capable of velocities up to 2.7 km/s (9,000 ft/s) on tracks as long as 13.3 km (50,781 ft) [14].

It is known that sled shoe-rail (slider-guider) contact is intermittent during a given sled run due to vibration and aerodynamic effects of the sled [1,4,6,7,15,23]. However, when the underside of the sled shoe and the rail do contact, high velocity, dry sliding interfaces are formed. A prominent feature of these interfaces is intense frictional heating which causes a temperature rise at the interface and in extreme cases can produce microstructural changes in the surfaces involved [6,7]. Studies have shown that rocket sled gouging occurs at locations where rocket sled shoes have been in contact with the rail surface [1,4,6,7,15,23].
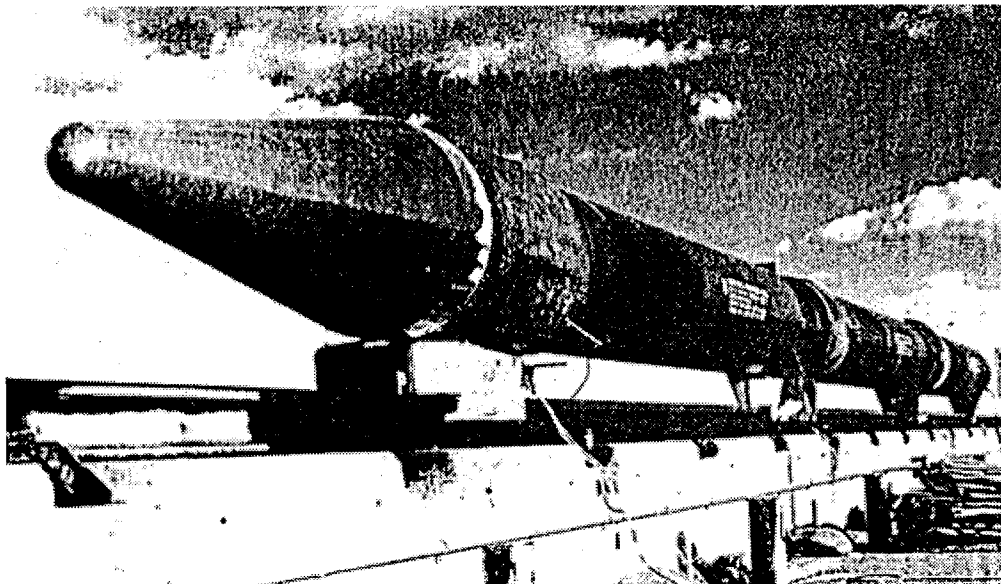
Figure 1.2: A Large Monorail Rocket Sled [15]

1.2.2 RAILGUNS

Railguns are electromagnetic accelerators that operate on the principle of Lorenz force. The interior of a railgun barrel is comprised of two parallel, opposing, conducting (usually copper) rails, separated by two parallel insulators, all extending the length of the barrel. Electric current supplied to the system flows down one rail, through an armature pushing a projectile or through the projectile itself, and back through the second rail. The current flowing in the rails produces a magnetic flux density between the rails and this magnetic field interacts with the current "I" flowing in the armature. The resulting IxB or Lorenz force accelerates the armature and/or projectile along the rails [16]. This is shown conceptually in Figure 1.3.
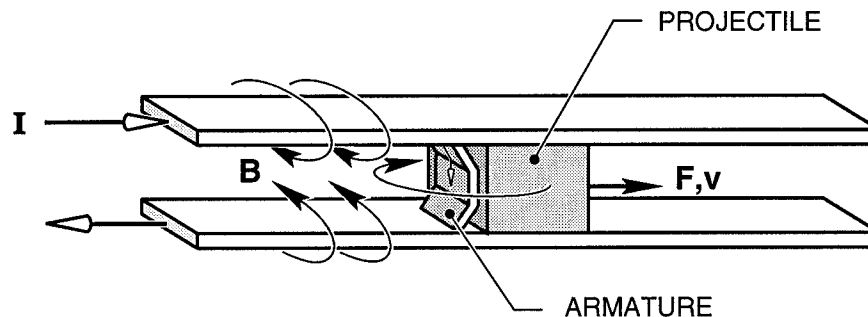
Figure 1.3: Principle of Railgun Operation

While forces produced in a railgun by currents in the kiloamp range aren't noteworthy, as current levels approach the megamp range, extremely large forces result [16].

6

Railguns have been used to launch projectiles with masses from a few to several thousand grams. Muzzle velocities in the 3 to 5 km/s (9,843 to 16,405 ft/s) are routinely achieved; muzzle velocities in excess of 7 km/s (22,967 ft/s) have been achieved by using a light gas gun to "inject" a projectile already traveling at a high velocity into the railgun [12].

Like the interface between a rocket sled shoe and the guiding rail, the interface between railgun armatures and rails is also generally one of dry sliding contact. However, the situation is made more complex by high current densities which flow through the interface. The Joule or ohmic heating that is generated by these current densities is known to contribute significantly to the temperature rise at the armature/rail interface [17-19].

1.2.3 TWO-STAGE LIGHT GAS GUNS

Two-stage gas guns operate much like a conventional gun in that a projectile is accelerated by expanding gas. In a conventional or "powder" gun, a projectile is accelerated by gases evolved through combustion of the propellant. In a two-stage gas gun however, propellant gases drive a piston which in turn compresses a "light gas", usually helium or hydrogen as shown in Figure 1.4.
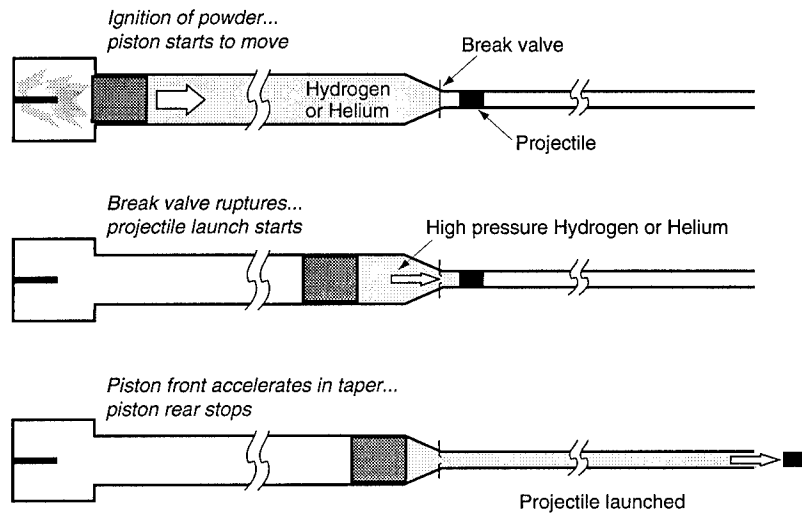
Figure 1.4: Two-Stage Gas Gun Principles of Operation (adapted from [20])

A diaphragm or rupture valve initially containing the light gas ruptures when the compressed gas exceeds the diaphragms design pressure, allowing the light gas to accelerate the projectile. The piston continues to push the gas until the lead portion of the piston, deformed by the conical, forward portion of the gas reservoir, slightly enters the launch tube of the gun, pushing the entire volume of expanding gas into the launch tube [21]. Two-stage gas guns are experimental devices used to generate projectile impacts at velocities in excess of 12.0 km/s (39,372 ft/s) [22].

CHAPTER 2

WORK CONDUCTED ON GOUGING TO DATE

2.1 REVIEW OF SELECTED PREVIOUS INVESTIGATIONS

In building the arguments that the onset of gouging is predictable and that gouging is possible at velocities lower than those previously reported, it is important to review past studies of the phenomenon. Many authors have made contributions to the study of hypervelocity gouging, the most recent being an investigation by Tachau reported in his 1991 doctoral dissertation at the University of Texas at Austin [2] and a follow-up paper presented at the 1994 Hypervelocity Impact Symposium [3]. The work of those authors whose contributions are most pertinent to this investigation of gouging is discussed and the highlights summarized below.

2.1.1 GRAFF, DETTLOFF, AND BOBULSKI, 1968, AND GRAFF AND DETTLOFF, 1969-70 - OHIO STATE UNIVERSITY [4,23,24]

Graff et al. felt that the basic nature of gouging was one of high-velocity sliding contact or grazing impact between metallic surfaces. A review of available technical literature revealed no observations or studies of the gouging phenomenon. However work done by Bowden and Freitag in 1958 [25] and Bowden and Persson in 1961 [26], the first comprehensive studies of high speed friction effects, was found to be relevant in terms of understanding the conditions at a rocket sled shoe - rail interface during gouging, as well as the problem of sled shoe wear.

9

Graff et al. catalogued data from gouge damage at the Holloman Air Force Base, New Mexico rocket sled test track. They found that sled velocity was the primary factor affecting the frequency of gouge occurrence. They also discovered that about 80% of the gouges were on the side or top edges of the rail head, 15% were on the undersides, and only 5% were on the top surface of the rail.

In an effort to duplicate gouging damage in a laboratory on a smaller scale and to evaluate several rocket sled shoe materials and rail coatings, Graff et al. designed experiments to create the conditions of high velocity sliding contact. A special gun facility was constructed that enabled them to shoot projectiles on a grazing angle of impact at a flat or curved target. The gun had a 6.0 ft (1.8 m) barrel with a 0.83 in (2.11 cm) bore and was capable of firing 7 to 60 gram (0.015 to 0.132 lbm) spherical or cylindrical projectiles at velocities from approximately 1.7 to 2.8 km/s (5,578 to 9,187 ft/s). Using this gun facility, initial attempts to produce gouges on target surfaces with a 20 ft (6.1 m) radius of target curvature and a 1 degree angle of projectile incidence proved unsuccessful. In order to increase the stresses at the projectile-target interface, the radius of curvature of the target surface was reduced to 3 ft (0.9 m). The projectiles were fired as closely as possible on a tangent to the curve to minimize initial contact damage. Using projectiles of brass, copper, steel, and aluminum with this sharply curved target surface, Graff et al. successfully created gouges on steel target surfaces that had all of the essential features of rocket sled rail gouges. Graff et al. initially found that gouges were more likely to occur at slight kinks in the curved projectile track, where normal forces were maximum, and that gouges were predictably

10

initiated at scratches and grains of sand deliberately placed on the track surface. In subsequent testing they found that all metallic projectiles caused gouging while Teflon did not, more noble metals gouged more, and harder metals had higher threshold gouging velocities.

2.1.2 GERSTLE, FOLLANSBEE, PEARSALL, AND SHEPARD, 1968-72 - DUKE UNIVERSITY [5,6]

In early 1968, Gerstle ran several monorail sled tests on the track at Sandia National Laboratories (SNL) with the specific goal of trying to initiate gouges on the rail. He found that gouges frequently occurred downstream from upward kinks in the rail but that a weld bead across the width of the rail did not cause gouging. A subsequent microanalysis of damaged portions of the rail (AISI 1080 Steel) revealed that gouges had a surface layer of martensite with a layer of 304 Stainless Steel (sled shoe material) deposited on top of the martensite. Examination below the surface of gouges showed that high enough temperatures had been reached to austenitize the steel, and that the rail material was severely strained and microcracked. This was all believed to be evidence of catastrophic thermoplastic shear (adiabatic slip). Cracks into the surface of gouges characteristically had stainless steel in their center surrounded by layers of martensite and then deformed pearlite. Rail surfaces that had not been contacted by sled shoes had no damage other than surface layer decarburization.

2.1.3 BARBER AND BAUER, 1982 - IAP RESEARCH [1]

Barber and Bauer contrasted sliding contact behavior at low velocity (less than 30 m/s (98 ft/s) and high velocity (less than 300 m/s (984 ft/s)) with that of hypervelocity which they described as the regime of velocity in which the predominant forces of interaction are inertial. They identified the existence of a hypervelocity "sliding threshold velocity" and also developed a model for the process of hypervelocity asperity impact and gouge formation. The following paraphrase from Barber and Bauer's work describes the interaction between two solid surfaces in frictional contact.

> When two solids are brought together, actual physical contact occurs at only a small number of discrete contact points. The normal load between the two solids is supported by these discrete areas. The number and size of the contact points increase with increasing applied load. Adhesion between two bodies in contact occurs at the contact spots and " cold welds" are formed. Tangential motion of one body with respect to the other deforms or shears material in the contact spots and results in further asperity contact. Frictional forces develop because of the ability of the contact spots to resist this deformation. (Wear results from material fracture due to excessive straining in the contact spot region.) During contact spot shearing, energy is dissipated into the deformation zone and then removed from

12

the deformation zone by thermal conduction into the material substrate.

As sliding velocity increases, the rate of energy dissipation in the deformation zone exceeds the conduction rate out of the deformation zone, causing the deformation zone temperature to rise. As sliding velocity increases still further, the temperature of the entire surface of a slider may reach the melting point, at which point a liquid interface is formed between the sliding surfaces, greatly reducing the frictional forces observed and the coefficient of friction. The liquid interface behaves as a hydrodynamic bearing. Viscoshearing of the liquid film dissipates energy which causes intense heating of the slider surface and results in surface melting. Surface recession occurs, providing an influx of melted material from the slider surface equal to the efflux from the interface due to slider motion, and a steady-state hydrodynamic interface is established. The development of this hydrodynamic fluid layer depends upon the material properties of the slider and guider, the sliding velocity, the normal load, and possibly the geometry of the slider.

At hypervelocity, if a fluid interface forms, velocity gradients in the interface will increase, as will the frictional force, energy deposition, surface recession, slider wear, and interface temperature. At some velocity, it is likely that the temperature of the interface region becomes so high that the

interface material is vaporized, with a resultant drop in viscosity and frictional force. If a fluid interface does not form, asperity contact continues to occur at very high velocities. The apserities, however, can no longer come into contact in a steady or quasi-steady mechanical mode. Instead, they impact generally in an oblique manner, generating shock stresses.

Barber and Bauer termed the point at which the impact-induced stress is equal to the ultimate strength of the material the "hypervelocity sliding threshold velocity." They felt that the hypervelocity sliding threshold velocity, as was impact stress, was related to the asperity impact velocity, the angle of impact, and the density and shock speed of the materials involved. They also felt that hypervelocity asperity impact would be a discrete, localized, violent event resembling a microscopic explosion that would be expected to produce a small crater in the surface of the material. The center of mass of this explosion would travel at approximately one-half of the slider velocity. Due to the relative motion of the slider, a tear-shaped crater would result rather than a simple, hemispherical shape.

Barber and Bauer found little quantitative data to support their theory. However, they felt that the conclusion drawn by Graff and Dettloff [4,23], generally that a minima of both sliding velocity and normal load were required to initiate gouging, confirmed the existence of a sliding threshold velocity. Additionally, they felt that instances of railgun rail gouging at the Australian National University (ANU) [1,47] further confirmed the existence of a threshold sliding velocity. It was felt that the onset of gouging, which

14

was experienced at the ANU at velocities as low as 300 m/s (962 ft/s), corresponded to the point at which asperity impact would produce stresses exceeding the ultimate strength of copper. It was also felt that the cessation of gouging at approximately 1.1 km/s (3,529 ft/s) corresponded to the full development of a fluid layer at the slider guider interface.

2.1.4 KRUPOVAGE, 1984 - HOLLOMAN AIR FORCE BASE [15]

In reviewing earlier work on gouging, Krupovage disagreed with the mechanism of gouging proposed by the Ohio State investigators [4,23]. He felt that omitting projectile-slider point-of-impact damage from consideration in the study of gouging was a mistake, stating that these impact regions should have been investigated further. He also pointed out that in addition to gouging, another rocket sled phenomenon observed to begin at velocities exceeding 1, 524 m/s (5,000 ft/s) was the loss of sled material in the forward area of the sleds due to aerodynamic heating.

After describing gouging experienced in a number of rocket sled runs with different sled types and test conditions, Krupovage concluded generally that rocket sled gouging is caused by debris which has become trapped in the sled slider (shoe) and rail interface and does not result solely from the load imparted to the rail through the slider. This debris was thought to originate either from a loss of slider and/or sled material due to aerodynamic heating or from sources external to the sled.

15

2.1.5 BARKER, TRUCANO, AND MUNFORD, 1987 - SANDIA NATIONAL LABORATORIES [8,9]

Barker et al., as did Graff and Dettloff [4,23] and Barber and Bauer [1], felt that gouging was an impact phenomenon and developed a theory and computer model accordingly. The theory of Barker et al. states generally that high pressure acts to deform the parallel (slider-guider) surfaces which impinge on each other in a continuous interaction that can produce gouges.

Barker et al. initially conducted a "parameter study" to try to quantify the physical conditions that must exist when gouging takes place and to verify the validity of assumptions made for the computer model. Among the findings of this parameter study were the following:

1. The frictional surface heating of a 30 mm (1.18 in) diameter steel projectile sliding at 3 km/s (9,843 ft/s) in a barrel with a nominal curvature of 1 mil per 10 in (25.4 cm) would be expected to result in surface melting of the projectile after 0.002 seconds (0.6 m (1.97 ft)) of travel and to a depth of 0.67 mm (0.026 in).

2. The impact of a steel asperity traveling at 2 km/s (6,562 ft/s) against a stationary steel asperity will generate a shock pressure of about 400 kbar (5,800 ksi), which is 40 times higher than the 150 ksi (10 kbar) yield strength of typical heat treated steel.

3. Based on a 6.0 km/s (19,686 ft/s) sound speed in steel and a 12.7 mm thick slider (sled shoe), it would take about 4.2 microseconds after an asperity impact for the first relief wave to arrive at the asperity (this is the round trip travel time of a sound wave from the asperity to the nearest free surface, i.e. the top of the slider/sled shoe). If the slider is traveling at 25 m/s (82 ft/s), the first pressure relief would come after about 1 mm of travel; if the slider is traveling at 2.0 km/s (6,562 ft/s), the first pressure relief would come after about 8.4 mm (0.33 in), of travel. Considering the higher pressures involved at the higher speed, it is not surprising that gouging does not occur at 25 m/s (82 ft/s) but may occur at 2.0 km/s (6,562 ft/s).

The gist of the parameter study was that at the conditions under which gouging may exist, because of the microasperity impact interaction between a slider and guider, extreme local deformation, heating, melting, and possibly vaporization may occur. Barker et al. suggested that this type of interaction would continue until the slider-guider gap increased enough to cause separation or until passage of the slider from the point of interaction. Their feeling was that conditions permitting, a microasperity impact would result in the development of a growing high-pressure interaction region. This would cause a self-sustaining reaction leading to the formation of a gouge. Barker et al. termed this "PIT" for Parallel Impact Thermodynamics.

Based on "PIT," Barker et al. developed and tested a two-dimensional model using the CSQ hydrodynamic computer code and a three-dimensional model using the CTH hydrodynamic computer code. To function properly,

17

the two-dimensional model required a gap between the slider and guider, and both the two and three dimensional models required a "gouge initiating asperity" and a normal load. The normal load was generated by giving the leading edge of the slider a 45 degree angle to impart downward motion to the asperity during impact. Barker et al. determined that both models confirmed the validity of "PIT."

By varying the simulation parameters, Barker et al. found that increasing the slider yield strength with respect to the guider, increasing the slider/guider separation distance, using a plastic slider, decreasing the "angle of attack" between the slider and guider, and decreasing the normal load between the slider and guider would all reduce the tendency to gouge. Based on these findings, Barker et al. designed a laminated rocket sled shoe comprised of alternating layers of plastic and high-strength, high-toughness steel and with a leading edge angle of 10 degrees. Backing steel with low density, low modulus plastic was intended to allow release waves to arrive earlier and decrease the pressure in a nucleating gouge before significant gouge growth occurred. Flexibility inherent in the design would provide some shock absorption, decreasing the peak normal pressure between the sled shoe and rail. The use of plastic layers was also intended to provide "melt lubrication" at high velocity.

A sled shoe using this design was subsequently tested on a small monorail rocket sled. The sled reached a velocity of 1.9 km/s (6,234 ft/s) and produced no rail gouges. Barker et al. felt that this validated the "PIT" theory.

2.1.6 SUSOEFF AND HAWKE, 1988 - LAWRENCE LIVERMORE NATIONAL LABORATORY [12]

Susoeff and Hawke compiled data on gouging damage that accumulated on a Lawrence Livermore National Laboratory 12 mm (0.47 in) diameter, round bore electromagnetic railgun. The gun had electrolytic tough pitch C11000 copper rails and was capable of launching 1 gram (0.0022 lbm) polycarbonate projectiles with foil armatures at velocities up to 6.6 km/s (21,655 ft/s). A helium preinjector was used to "inject" the projectiles with an initial velocity of 1.0 to 1.2 km/s (3,281 to 3,937 ft/s) into the railgun breech prior to the addition of electrical energy.

Susoeff and Hawke found that existing gouges grew larger and deeper after subsequent experimentation and that sometimes additional gouging damage sites would form "upstream" or "downstream" of the original damage. They also determined from visual inspection that more electrical energy (resulting in higher pressure) seemed to result in larger initial gouges. An evaluation of gouge data as a function of projectile velocity indicated that areas of concentrated damage generally occurred at velocities of between 1.5 and 2.5 km/s (4,922 and 8,203 ft/s) with isolated gouges occurring at velocities from 1.2 to 6.6 km/s (3,937 to 21,655 ft/s).

Modifying the projectiles to include transverse fins proved to be key in eliminating bore damage due to gouging. In five subsequent experiments, finned polycarbonate projectiles achieved velocities from 4.5 to 7.4 km/s (14,765 to 24,279 ft/s) without causing gouging.

19

2.1.7 BARKER, TRUCANO, AND SUSOEFF, 1989 - SANDIA NATIONAL LABORATORIES AND LAWRENCE LIVERMORE NATIONAL LABORATORY [10,11]

Barker et al. reviewed the data collected in Susoeff and Hawke's 1988 report [12] and then acknowledged that the source of gouging damage was still uncertain; the experiments that had produced gouging were designed to improve railgun performance rather than to study gouging. Barker et al. suggested that the gouging damage may have been caused by molten droplets of the aluminum commutator "impinging" at low angle into the rails and "digging in." Barker et al. reasoned that the higher energy levels used on the last five shots (with finned projectiles) likely resulted in complete vaporization of the aluminum commutator and thus no gouging whereas earlier shots that produced gouging did so because of incomplete vaporization of the foil.

Barker et al. used the "PIT" theory to conduct a CTH hydrodynamic code parameter study to predict the conditions under which gouging can occur. In the study, they evaluated all possible slider-guider combinations of copper, steel, aluminum, and plastic at velocities from 0.5 to 12.0 km/s (1,641 to 39,372 ft/s). The results were examined to determine whether the initial microasperity impact at a slider-guider interface would result in a growing, stable or decaying interaction region; a growing interaction region would indicate the formation of a gouge. Barker et al. determined that materials which can gouge each other do so only within a certain range of velocities. They also determined the following:

1. There are both upper and lower gouging threshold velocities; the upper threshold velocity has never been experimentally observed.

2. When sliding exceeds twice the wave velocities of the interacting materials, gouging does not occur. This is apparently because there is insufficient time for material to be continually pushed up in front of the interaction zone and the reaction dies out.

3. Higher yield strengths raise the lower gouging threshold (and may lower the higher threshold as well).

4. Computer calculations infer that a nearly steady "stream of gas" emanates from the leading shoulder of plastic sabot projectiles because of shock vaporization due to micro impacts (what is normally ascribed to blow-by).

5. A 10 degree "angle of attack" on the slider will reduce the "stream of gas" and the tendency for gouging to occur.

2.1.8 TACHAU, 1991 - THE UNIVERSITY OF TEXAS AT AUSTIN, AND TACHAU, YEW, AND TRUCANO, 1994 - SANDIA NATIONAL LABORATORIES AND THE UNIVERSITY OF TEXAS AT AUSTIN [2,3]

Tachau improved upon the "PIT" theory presented by Barker et al. in 1987 and 1989 [8-11] by eliminating the gap between the slider and guider as well as the required "gouge initiating asperity" from the CTH computer

model. Instead, an initial slider velocity component normal to the sliding surface was applied to the model. Tachau felt that this would result in the development of "antisymmetric humps" as described by Abrahamson and Goodier in 1961 [27].

Abrahamson and Goodier observed that as a hump deformation is driven in front of a rolling pin when a slab of bread dough is being rolled out, humps precede moving loads on layers of soft or viscous material. They concluded that this antisymmetric behavior is the result of inelastic behavior of the layer. If the material were elastic, the deformation would be symmetrical with equal bumps upstream and downstream of the load. For a stationary viscous material, the surface profile changes due to penetration of the load. If the penetration is stopped and the material is given a horizontal velocity, the leading hump is drawn by convection under the penetrating load. The actual profile then, is determined by the combination of penetration and convection. For a symmetric loading of an incompressible material, the surface displacement, which is significant only near the load, creates the characteristic hump.

Tachau suggests that as the temperature increases during sliding, the contact surface becomes very hot and the normally elastic material begins to behave like a viscoplastic material. Then, when obliquely impacted, the shallow heated zone of softened material allows the formation of antisymmetric deformations as described above. Since both the slider and the guider become very hot, antisymmetric deformations would be expected to form on both contact surfaces. If conditions permit a continuous interaction

22

of the heated, viscous layers, a gouge would be initiated in a manner similar to the "PIT" model described by Barker et al. [8,9].

Tachau conducted CTH hydrocode computer simulations (with ANEOS equations of state) for a slider and guider both made of steel. He found that a slider with an initial horizontal velocity of 2.0 km/s (6,562 ft/s) and downward velocity of 0.1 km/s (328 ft/s) did cause gouging but that a slider with an initial horizontal velocity of 1.0 km/s (3,281 ft/s) and downward velocity of 0.1 km/s (328 ft/s) did not cause gouging. These results led him to conclude that:

1. The temperature at the contact surface must be sufficiently high to cause the materials at and near the contact surface to become viscoplastic.

2. The impact condition must be severe enough to ensure the creation of a growing, high-pressure core at the contact surface.

Tachau went on to suggest that the threshold gouging velocity for high-speed guns is substantially higher than that experienced in rocket sled testing because of differences in mechanical tolerances inherent in the systems. Specifically, in high-velocity guns, the barrel is accurately machined and aligned and the projectile is carefully balanced. Thus, the magnitude of impulse produced by any projectile unbalance or barrel misalignment is small compared to that which occurs in rocket sled tests. Recommendations to mitigate gouging included carefully aligning entire slider-guider systems,

designing sliders for aerodynamic stability, and eliminating slider-guider contact while minimizing slider-guider clearance.

2.2 CONSOLIDATION OF FINDINGS

In the work on gouging done to date, the causes to which gouging has been directly attributed include the following:

1. Debris on guider [12]

2. Balloting motion/vibration of the slider against the guider [12]

3. Slider break-up during acceleration [12]

Other suggested mechanisms that lead to or result in gouging include:

4. Catastrophic Thermoplastic Shear [5,6]

5. Hypervelocity microasperity impact between the slider and guider contact surfaces [1]

6. Shock induced pressure accumulation at the slider-guider interface

7. Parallel Impact Thermodynamics (PIT) [8-11]

8. Viscoplastic materials at the contact surfaces [2]

Despite the variety of causes and mechanisms suggested and the three different systems involved, there are common threads in these findings. Slider velocity, stresses at the contact surface as a function of slider normal force, and material properties of the slider and guider are repeatedly identified as important factors that determine if gouging will occur. Whether imposed by asperity impacts or the contact between deformed slider and guider surface layers, it is generally agreed that some minimum amount of

normal force at a slider-guider interface, relative to the properties of the materials involved, is likely required for gouging to occur. It seems that if the normal forces at a slider-guider interface lead to an accumulation of shock induced pressure at the point of contact, phase transformations, softening, melting, and possibly vaporization and gouging of both slider and guider surfaces may occur.

2.2.1 TENDENCY TO GOUGE

Graff and Dettloff [4,23] identified that slider velocity was the primary factor affecting the frequency of gouge occurrence and that gouges were more likely to occur where normal forces were at a maximum. The simulations of Barker et al. [8-11] demonstrated the importance of a normal load for gouging to occur at a certain velocity through the need of a "gouge initiating asperity." They also showed that increasing slider yield strength with respect to the guider reduced the tendency to gouge. Tachau's simulations [2] confirm the importance of velocity and normal load in that some combination of the two is required for gouging to occur. Based on these findings, slider velocity and slider normal force with respect to the guider must be critical factors that determine whether or not gouging will occur for a given set of materials.

2.2.2 SUITABLE MATERIAL COMBINATIONS

Graff et al. [23] found that every metal-on-metal combination they tested produced laboratory gouges while plastic-on-metal combinations did not, and that prevention of metal to metal contact prevented gouging. They also noted that more noble metals seemed to gouge more. With the exception of one instance mentioned by Barker et al. [8,9] of Lexan producing gouges at a barrel joint, all reported occurrences of gouging involved metal sliders and metal guiders. The simulations by Barker et al. [10,11] indicated that all metal-on-metal combinations tested would produce gouging at certain velocities while plastic-on-metal combinations would not cause gouging at any velocity. It seems safe to say then, that gouging is almost exclusively a metal-on-metal phenomenon.

2.2.3 THE GOUGING ONSET VELOCITY AND GOUGING "WINDOWS"

The gouging threshold or gouging onset velocity is the lowest sliding velocity at which gouges begin to appear. Barber and Bauer [1] termed this the "hypervelocity sliding threshold velocity" and described the situation there as the point at which the stress induced by the impact of the slider and guider surface asperities equaled the ultimate strength of the material. They thought that the location of this point was a function of the angle of asperity impact and the density and shock wave speed of the materials involved. Graff et al. also noted the existence of threshold gouging velocities. They found that harder metal sliders had higher threshold gouging velocities [24].

26

The simulations of Barker et al. [10,11] likewise indicated the presence of gouging onset velocities. In addition, they indicated that for a given set of material properties and conditions, materials which can gouge each other do so only within a certain range of velocities. Further, Barker et al. found that "higher yield strengths raise the lower gouging threshold and may lower the high velocity threshold as well" [11], though it is unclear whether they are referring to the slider material or instead the guider material. Barker et al. felt that experimental instances of steel-on-steel gouging supported their findings regardless of the fact, as they stated, that "the upper threshold has never been observed" [11].

In actuality though, lower and upper gouging threshold velocities have been experimentally observed. Barber and Bauer [1] reported that lower and upper gouging threshold velocities of 300 m/s (984 ft/s) and 1.1 km/s (3609 ft/s), respectively had been experienced with copper in experiments at the ANU.

2.2.4 THE NATURE OF GOUGING

Based on previous findings, there theoretically exists for many metals and metal combinations a range or "window" of gouging velocities inside of which gouging will occur and outside of which it will not occur. The location of this "window" is a material dependent property, at a minimum being a function of the material strength and hardness. It seems reasonable then, that given the proper conditions and materials with appropriate properties, gouging is possible at velocities other than those at which it has previously been observed.

27

CHAPTER 3

THE FEASIBILITY OF GOUGING AT LOW RELATIVE VELOCITIES

Gouging has been categorized as strictly a hypervelocity phenomenon, one that is in "the regime of velocity in which forces of interaction are predominantly inertial" [1], that is, where inertial forces dominate over those deriving from strength of materials. The conditions of hypervelocity are generally considered to occur at sliding velocities greater than 1 km/s (3,281 ft/s). It must be recognized though, that hypervelocity is a relative term with respect to the properties of the materials involved. This is to say that the hypervelocity regime for steel may not be the same as the hypervelocity regime for some other material with substantially less strength and density. For this reason, with the correct choice of material(s), it should be possible to create the conditions of hypervelocity at velocities well below 1 km/s (3,281 ft/s). Likewise, given the proper conditions and a material or materials that are prone to gouge, it seems reasonable to expect gouging and its onset to occur at velocities lower than those at which it has been previously observed.

3.1 THE CORRELATION BETWEEN THE GOUGING ONSET VELOCITY AND MATERIAL PROPERTIES

As previously discussed, it has been found that the onset of laboratory produced gouging can be delayed by increasing material hardness [4,23]. Similarly it has been found that the onset velocity of simulated gouging can be increased by increasing material yield strength [10,11]. These findings are in agreement as penetration hardness has been shown both theoretically and

28

experimentally to vary linearly with yield strength for pure metals, alloys, and many non-metals [28]. It has also been found that gouging would be expected to occur at the velocity at which asperity impact-induced stress is equal to the ultimate strength of a material [1].

These findings indicate a strong correlation between gouging onset velocity and material strength properties. Whether this relationship involves slider materials, guider materials or both, though, is unknown. It is also uncertain if this relationship holds true for all gouging occurrences. The existence of the same correlation drawn from documented instances of gouging provides a much more convincing argument for the relationship between material strength properties and gouging onset velocity.

3.1.1 DOCUMENTED INSTANCES OF GOUGING

There are relatively few documented instances of gouging. Where gouging has been discussed, details of interest to the gouge researcher are often absent. In saying this though, it is understood that:

1. Gouging has probably occurred many more times than have ever been recorded.

2. When gouging has occurred, it has been inadvertent and not the intended purpose of the research or experiment.

29

3. Recorded discussions of a single instance of gouging are often representative of many occurrences over a period of time. For example, railgun gouging has occurred numerous times and still frequently occurs, but each instance is not individually recorded.

The instances of gouging reflected in Table 3.1 represent the majority of recorded discussions of the phenomenon.

SYSTEM	GOUGING ONSET VELOCITY km/s (ft/s)	SLIDER MATERIAL	GUIDER MATERIAL	DATE	AUTHOR	SOURCE(S)
ROCKET SLED						
Monorail	1.585 (5200)	AISI 304	AISI 1080	1968	Graff and Dettloff	[1]
Monorail	1.61 (5282)	AISI 4340	AISI 1080	1968	Krupovage	[15]
Monorail	1.524 (5000)	AISI 304/17 PH	AISI 1080	1972	Gerstle et al.	[5,6]
Monorail	2.438 (8000)	Vascomax 300	AISI 1080	1982	Krupovage	[15]
Monorail	1.859(6100)	AISI 4130 w/ Copper Wedge	AISI 1080	?	Krupovage	[15]
GUN						
Powder	Unknown	Numerous	Steel	1969	Graff and Dettloff	[4,23]
Rail	0.30 (984)	OFHC Copper	OFHC Copper	1972	Barber and Bauer	[1]
Rail	0.60 (1969)	OFHC Copper	OFHC Copper	1977	Marshall	[47]
Two-Stage Gas	3.000 (9843)	Lexan/Tantalum	AISI 4330	1987	Barker et al.	[8,9]
Two-Stage Gas	4.000(13124) @ Barrel Joint	Lexan	AISI 4330	1987	Barker et al.	[8,9]
Rail	1.200 (3937)	Polycarbonate	C11000 Copper	1987	Susoeff and Hawke	[12]
Rail	1.400 (4593)	Al 7075-T6	ETP Half-hard Copper	1994	Marshall	[29]

Table 3.1: Documented Instances of Experimental Gouging

3.1.1 INSTANCES OF SIMULATED GOUGING

With the assumption that they are viable models of the phenomenon, computer simulations which "result" in gouging are also useful source of gouge data. These are reflected in Table 3.2.

SYSTEM	GOUGING ONSET VELOCITY km/s (ft/s)	SLIDER MATERIAL	GUIDER MATERIAL	DATE	AUTHOR	SOURCE(S)
SIMULATION						
CTH	0.750 (2461)	Copper	Copper	1987	Barker et al.	[10,11]
CTH	1.750 (5742)	Steel	Copper	1987	Barker et al.	[10,11]
CTH	2.500 (8203)	Aluminum	Copper	1987	Barker et al.	[10,11]
CTH	1.750 (5742)	Steel	Steel	1987	Barker et al.	[10,11]
CTH	3.750 (12304)	Aluminum	Steel	1987	Barker et al.	[10,11]
CTH	1.750 (5742)	Aluminum	Aluminum	1987	Barker et al.	[10,11]
CTH	Unknown	Steel	Steel	1991	Tachau	[2]

Table 3.2: Documented Gouging Simulations

3.1.3 SUITABILITY OF DATA FROM DOCUMENTED INSTANCES OF GOUGING

Data suitable for the purpose of drawing a believable correlation between the onset of gouging and material properties must reflect a gouging occurrence where the gouging onset velocity, slider material, and guider material all are identified. Additionally, the instance of gouging must have occurred after a period of somewhat sustained contact between the slider and guider bulk materials as opposed to a sudden, unexpected material interaction. Otherwise, it is uncertain whether the gouging occurred at the

31

material(s) gouging onset velocity or merely at the point where materials already within their "gouging window" came into contact with each other. Accordingly, all of the instances of gouging reflected above do not lend themselves to a gouging onset velocity - material property analysis. Further, some of the instances shown have identical slider-guider combinations but different gouging onset velocities. Others reflect identical sliders with different guiders and different gouging onset velocities. In these situations, the lowest value of velocity has been considered the gouging onset velocity for that slider-guider combination or slider, respectively. For these reasons, only the **bold print** entries in Tables 3.1 and 3.2 above were considered further in the analysis of gouging which follows.

3.1.4 MATERIAL PROPERTIES OF SLIDERS AND GUIDERS FROM DOCUMENTED INSTANCES OF GOUGING

Collecting material properties data for gouging materials is a difficult process. There is no single source where all desired properties of the materials of interest can be found. Even when desired properties are located, they are often listed in units requiring conversion or for differing temperature ranges. Further compounding the problem is the fact that for virtually all recorded instances of gouging, some deductive reasoning is required to determine the specific type of material involved; without hardness or heat treating information, the properties of a material such as "Steel" or "Maraging Steel" must be approximated. In spite of these difficulties, properties for all gouging materials were collated. Reflected in Table 3.3 are strength and hardness properties of the materials from recorded instances of gouging.

These and numerous other properties are tabulated and their sources identified in Appendix A. In instances where the slider consisted of two different materials and additional evidence suggested that only one of the materials was involved in the gouging, this one material is listed as the slider material. In situations where the material property had a range of possible values, the median value is listed. Room temperature values are reflected for temperature dependent properties.

SYSTEM	SLIDER MATERIAL	GUIDER MATERIAL	GOUGING ONSET VELOCITY km/s (ft/s)	SLIDER YIELD STRENGTH MPa (ksi)	SLIDER DENSITY g/cm^3 (lb/in^3)	GUIDER YIELD STRENGTH MPa (ksi)	GUIDER DENSITY g/cm^3 (lb/in^3)
Rocket Sled	AISI 304	AISI 1080	1.524 (5000)	655 (95)	7.89 (0.017)	620 (90)	7.84 (0.017)
Rocket Sled	AISI 4340	AISI 1080	1.610 (5282)	841 (122)	7.85 (0.017)	620 (90)	7.84 (0.017)
Rocket Sled	Vascomax 300	AISI 1080	2.438 (8000)	1447 (210)	8.00 (0.018)	620 (90)	7.84 (0.017)
Railgun	OFHC Copper	OFHC Copper	0.300 (984)	217 (31)	8.92 (0.020)	217 (31)	8.92 (0.020)
Railgun	Polycarbonate	C11000 Copper	1.200 (3937)	72.5 (11)	1.19 (0.003)	310 (45)	8.89 (0.020)
Railgun	Al 7075-T6	ETP Half-hard Copper	1.400 (4593)	503 (73)	2.80 (0.006)	250 (36)	8.89 (0.020)
Simulated	Copper	Copper	0.750 (2461)	100 (15)	8.94 (0.020)	100 (15)	8.94 (0.020)
Simulated	Steel	Copper	1.750 (5742)	700 (102)	7.85 (0.017)	100 (15)	8.94 (0.020)
Simulated	Steel	Steel	1.750 (5742)	700 (102)	7.85 (0.017)	700 (102)	7.85 (0.017)
Simulated	Aluminum	Aluminum	1.750 (5742)	300 (44)	2.70 (0.006)	300 (44)	2.70 (0.006)

Table 3.3: Yield Strength and Hardness of Sliders and Guiders From Documented Instances of Gouging

3.1.5 A COMPARISON BETWEEN GOUGING ONSET VELOCITY AND YIELD STRENGTH

In an attempt to find a correlation from experimental data which validated the apparent relationship between material strength and gouging onset velocity, all of the properties reflected in Table 3.3 and Appendix A

were plotted individually against the values listed for the onset of gouging. This was done for all possible combinations of experimental data, simulated data, sliders only, guiders only, and sliders and guiders together. The only apparent relations revealed were between slider yield strength and gouging onset velocity and similarly between slider hardness and gouging onset velocity. Plotted in Figure 3.1 with a linear curve fit is slider yield strength versus gouging onset velocity for six instances of experimental gouging.
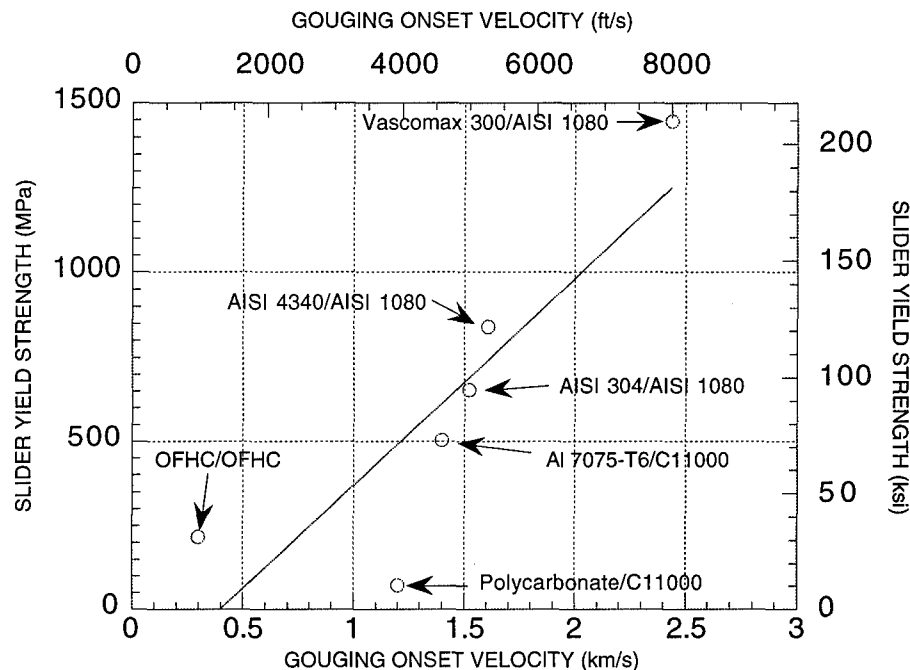
Equation of Linear Curve Fit: y = -242.42 + 612.68x (R = 0.86)

Figure 3.1: Slider Yield Strength versus Experimental Gouging Onset Velocity (Slider Material/Guider Material)

In spite of the limited number of data points, there does appear to be a correlation between gouging onset velocity and slider yield strength.

Combining data from simulated instances of gouging data with experimental data yields the plot in Figure 3.2. Again, for instances that reflected the same slider-guider material combination but different onset velocities, the lowest value of velocity was considered the gouging onset velocity for a slider of that material. Here, a linear correlation between gouging onset velocity and slider yield strength is more apparent though the data points are still somewhat scattered.
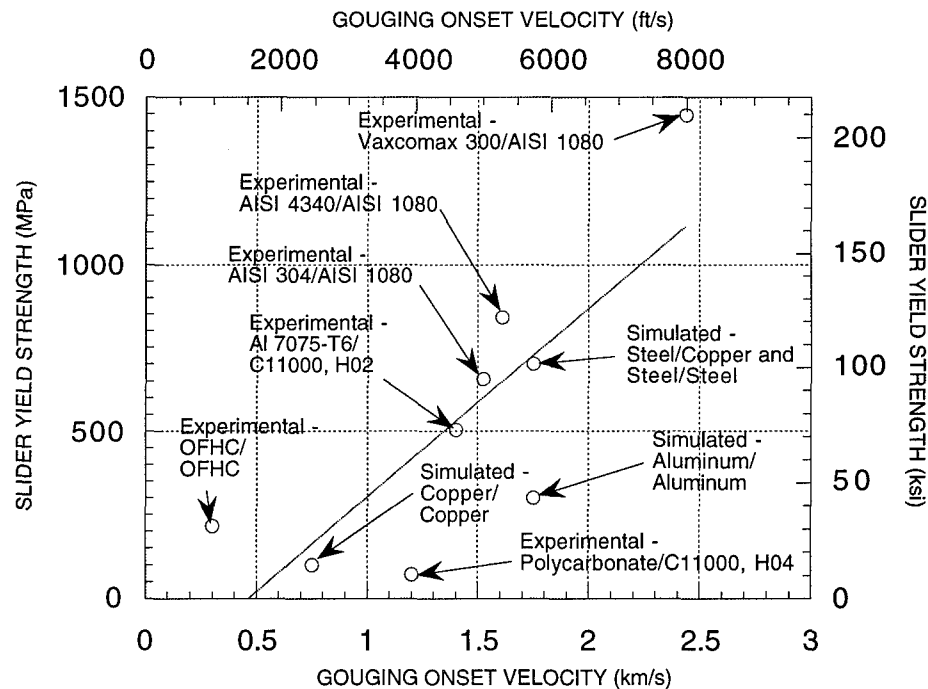
Equation of Linear Curve Fit: $y = 1261.72 + 565.25x$ $(R = 0.80)$

Figure 3.2: Experimental and Simulated Slider Yield Strength versus Gouging Onset Velocity (Slider Material/Guider Material)

In an attempt to draw the data points closer to the linear curve fit, the data was further manipulated by dividing slider yield strength by slider density. The curve fit was also extrapolated to the axis limits. The result is shown in Figure 3.3.
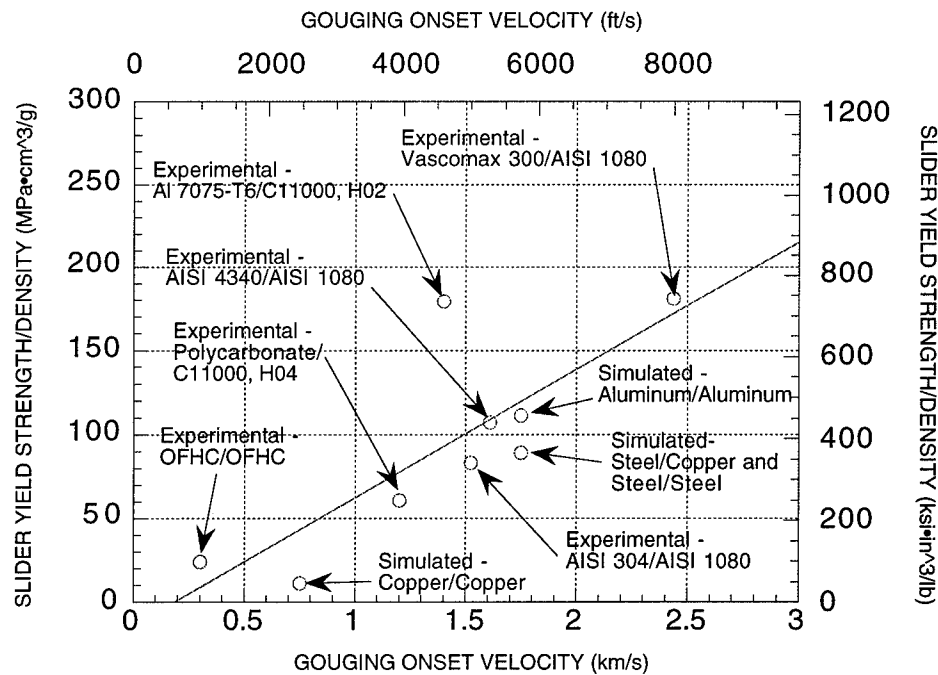
Equation of Linear Curve Fit: y = -13.76 + 76.31x (R = 0.79)

Figure 3.3: Experimental and Simulated Slider Yield Strength/Density versus Gouging Onset Velocity (Slider Material/Guider Material)

Here a linear correlation is visibly most evident. Even though the correlation coefficient (R = 0.79) is less than ideal, this plot tends to confirm that there is a connection material strength and the onset of gouging. Specifically, experimental data has been used to demonstrate a linear correlation between gouging onset velocity and slider yield strength.

36

3.2 THE FEASIBILITY OF CREATING HIGH VELOCITY PHENOMENA AT RELATIVELY LOW VELOCITIES

After establishing a linear correlation between slider yield strength and gouging onset velocity, it is possible to predict the gouging onset velocity of chosen slider materials. Extrapolating this relation to the axis lower limit makes possible the prediction that gouging could occur at low relative velocities, velocities which are well below those at which gouging normally occurs, with the proper selection of a slider material.

The fact that other high velocity surface effects between two materials have been reproduced at or scaled to lower velocities supports the believability of such an extrapolation. One example of this can be found in oblique impact experiments where steel bullets striking a thin sheet of lead at a particular angle of incidence (and then penetrating the sheet) produced wave-like surface deformations on the face of the bullet. These same deformations, similar to those formed during explosive welding, were subsequently reproduced on the surfaces of heavy automotive grease and silicon putty with a water jet operating at a much lower velocity [30].

Shooting projectiles at a curved surface, a technique pioneered at Ohio State University, is a proven method of producing gouges in the same realm of sliding velocities where gouging has been found to inadvertently occur [4,23]. In the Ohio State study, projectile impact velocities ranged from 1,524 to 2,438 m/s (5,000 to 8,000 ft/s). It seemed reasonable that the same or a similar method could be used with scaled data from the newly established linear relation to produce laboratory gouges at sliding velocities lower than those at which gouging had previously been observed.

37

CHAPTER 4

DEVELOPING AN EXPERIMENT TO PRODUCE GOUGES

A laboratory experiment with a three-fold purpose was devised to replicate the gouging phenomenon. First, it was intended to confirm the apparent correlation in reported instances of gouging between velocity and slider strength/hardness and the corresponding extrapolation to lower relative velocities. It was further intended to pinpoint the gouging onset velocity for a chosen material and a given set of conditions. Lastly, was it intended to create gouges inexpensively and in a manner that could be readily duplicated.

4.1 EXPERIMENTAL SET-UP

With the existence of a previously successful method of producing laboratory gouges, replication of this method seemed a logical approach to accomplishing the stated goals. Shooting projectiles at a curved surface seemed fundamentally easy to accomplish even though the actual gun and experimental set up used at Ohio State was rather specialized [23].

By using an experimental .22 caliber light-gas pellet gun, a chronograph to measure projectile velocity, and section of steel cylinder as a target form and catch tank, an experimental set-up similar to that which was used at Ohio State was built [23]. This set-up though, also designed to produce gouges by shooting projectiles at a curved surface, was likely

38

constructed with far less effort and expense. The setup of this experiment is shown in Figure 4.1.
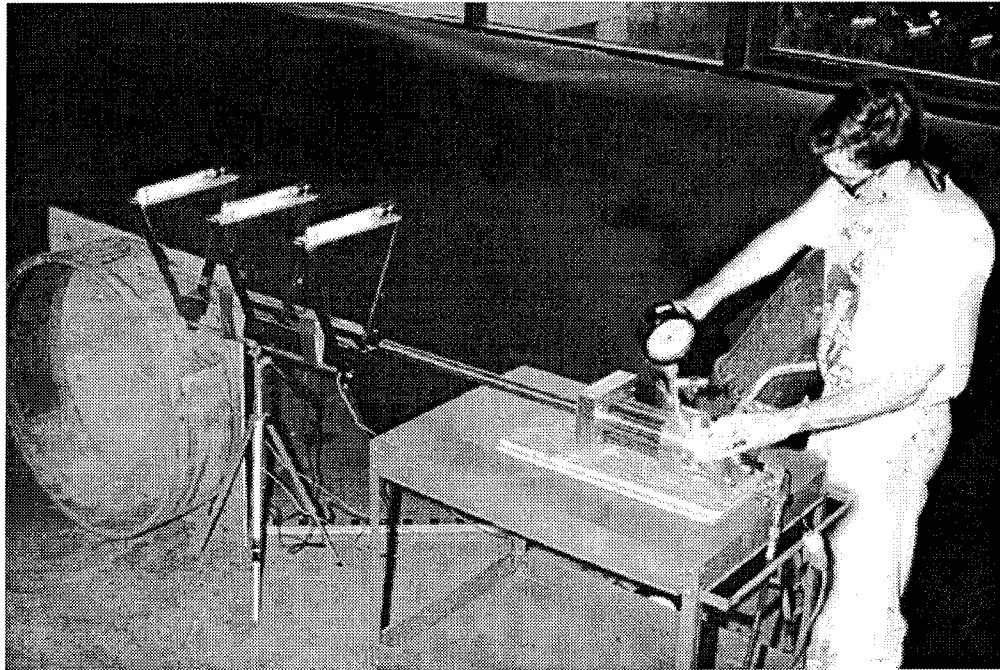
Figure 4.1: Experimental Setup for Low Relative Velocity Gouging

4.1.1 BUILDING A LIGHT-GAS PELLET GUN

It was desired to use standard, commercially available items where possible in this experiment so that a maximum effort could be focused on creating gouges as opposed to building the experiment. Safety considerations dictated that a .22 caliber gun or smaller be used to accelerate "sliders." Further it was desired to be able to accelerate "sliders" to a range of possible velocities so that if gouges were created, slider velocity could be reduced

gradually and the gouging onset velocity for the material(s) used could be isolated. Additionally, a smooth-bore gun was desired so that any effect created by a projectile-slider accelerated by the gun would not unknowingly be caused by spinning of the slider. The obvious approach to accomplish all of this was to purchase a pump air rifle. Unfortunately, the very best air rifles commercially available offer a maximum muzzle velocity of approximately 335 m/s (1100 ft/s). As the likelihood of producing gouges at low relative velocities was still somewhat uncertain, being restricted to a maximum possible sliding velocity this low was less than desirable. Accordingly, an experimental light-gas gun was built that could fire a standard size .22 caliber pellet at higher muzzle velocities.

An existing 643.53 cm^3 (39.27 in^3) aluminum pressure cylinder was modified to mate with a 63.5 cm (25.0 in), .22 caliber, chrome-molybdenum barrel blank purchased from Douglas Barrels, Inc. of Charleston, West Virginia. The rim-fire barrel had a smooth bore, having been reamed but not rifled, with an inner diameter of 5.54 mm (0.2183 in) and an outer diameter of approximately 3.81 cm (1.50 in). Already attached to and passing through the pressure cylinder was a lance used to rupture mylar diaphragms of varying thickness placed between the tapered outlet of the pressure cylinder and the breach face of the barrel, thus allowing high-pressure gas to flow from the cylinder into the barrel. The lance, attached to an enclosed piston, was operated using 690 kPa (100 psi) air (standard shop air pressure) and activated by opening an electrically actuated solenoid valve. The gun is shown in Figure 4.2.
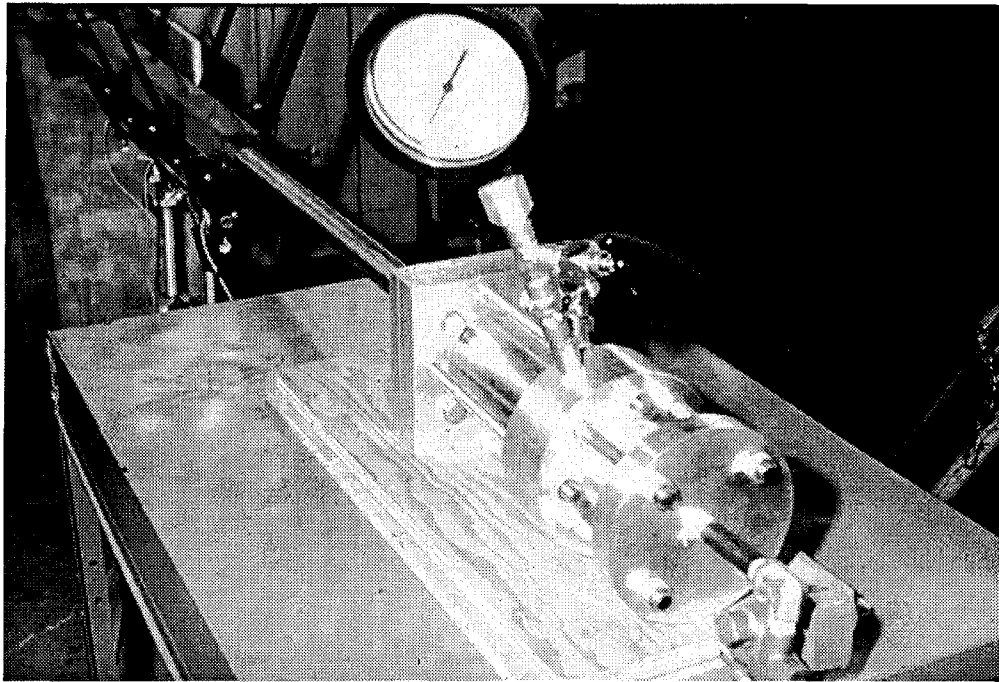
Figure 4.2: Experimental .22 Caliber Light Gas Pellet Gun

Helium was used as the accelerating gas for the gun. By regulating a standard 6.12 m^3 (216 ft^3) cylinder of helium purchased from a local welding supply company, the gun chamber pressure could be varied from ambient pressure up to about 13.79 MPa (2,000 psi), the approximate maximum pressure of a "full" cylinder of helium. An assembly with a check valve, a pressure gauge, and a relief valve attached to the gun chamber provided readings to an accuracy of 69.0 kPa (10 psi) of chamber pressure as it was increased (prior to firing the gun). It also maintained the reading of the maximum pressure attained in the chamber until the relief valve was opened (after firing the gun).

A rough estimate of gun performance was determined by conducting a simplified fluid dynamics analysis of the system to determine the combined static and dynamic fluid effects of helium on a projectile. The dynamic fluid effects can be determined by modeling the gun chamber and barrel assembly as a convergent nozzle, as shown in Figure 4.3.
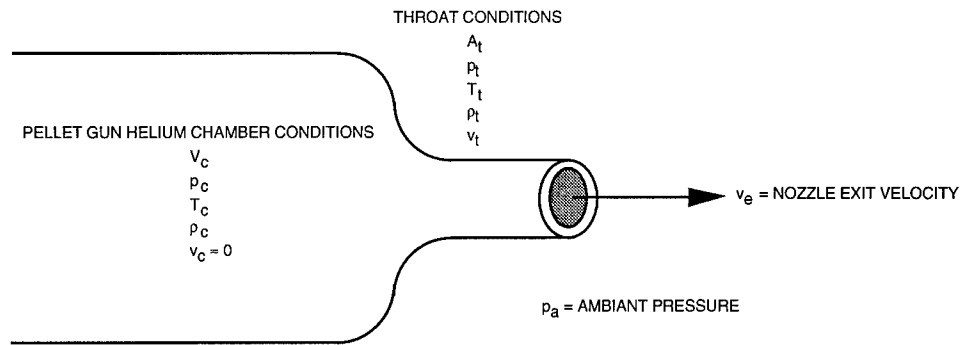
Figure 4.3: Idealized Gun Pressure Chamber and Barrel Assembly
(adapted from [31])

The flow through the throat of a convergent nozzle will either be sonic or subsonic, as determined by [31]:

$$\frac{p_t}{p_c} = \left(\frac{2}{k+1}\right)^{\frac{k}{(k-1)}}$$

(4.1)

where p_c = initial chamber fluid absolute pressure

             p_t = absolute throat pressure

             k = ratio of specific heats for helium

For helium, k = 1.66 and:

$$\frac{p_t}{p_c} = \left(\frac{2}{1.66+1}\right)^{\frac{1.66}{(1.66-1)}} = 0.4881 \qquad (4.2)$$

Flow through the nozzle will be sonic if p_c is critical such that:

$$0.4881 > \frac{p_a}{p_c} \qquad (4.3)$$

where $\qquad$ p_a = ambient pressure

If p_a is assumed to be 14.7 psia (101.3 kPa), for any value of p_c greater than 30.1 psi (207.7 kPa), nozzle flow will be sonic and:

$$p_t = (p_c)(0.4881) \qquad (4.4)$$

For sonic flow, the nozzle is "choked" and the nozzle throat velocity v_t will be a maximum, characterized by the equation [32]:

$$v_t = v_e = v_{max} = \left(\frac{2k}{k+1} RT_c\right)^{\frac{1}{2}} \qquad (4.5)$$

where: $\qquad$ T_c = absolute temperature of chamber fluid, assumed to be $530^{\circ}R$

$\qquad\qquad$ R = gas constant = 12,420 $\dfrac{ft^2}{(s^2 \bullet\, ^0 R)}$ for helium [32]

With the values as shown:

$$v_t = v_{max} \approx 2866 \text{ ft/s} \tag{4.6}$$

From v_t, the dynamic fluid energy imparted to a projectile can be determined. If it is assumed that only half of the original mass helium in the chamber is accelerated, the dynamic energy imparted to the projectile E_d is equal to:

$$E_d = \frac{1}{2} m_{\substack{accelerated \\ aas}} v_t^2 \tag{4.7}$$

where:

$$m_{\substack{accelerated \\ gas}} = \frac{1}{2} \left[\frac{\left(p_c \frac{lb}{in^2} \right) \left(144 \frac{in^2}{ft^2} \right) \left(V_c in^3 \right) \left(\frac{1ft^3}{1728 in^3} \right)}{RT_c} \right] \text{slugs} \tag{4.8}$$

$$V_c = \text{chamber volume} = 39.27 \text{ in}^3$$

Equation 4.7 reduces to:

$$E_d = 1.02 p_c \text{ ft-lbf} \tag{4.9}$$

Assuming the projectile is initially in the nozzle throat, the static energy imparted to the projectile can also be calculated directly from p_c and

44

Equation 4.4. If the cross sectional area of the projectile is assumed to be equal to A_t, the force of p_t on the projectile will be:

$$F_{p_t} = (p_c)(0.4881)(A_t) \text{ lbf} \qquad (4.10)$$

where: $\quad A_t$ = nozzle throat area = $\dfrac{\pi}{4}(0.2183 \text{in})^2 = 0.0374 \text{in}^2$

and

$$F_{p_t} = (1.83 \times 10^{-2})(p_c) \text{ lbf} \qquad (4.11)$$

Though in actuality it is not, if F_{p_t} is assumed constant over the length of the barrel "l" during which it acts on the projectile, the energy imparted to a projectile from F_{p_t} will be:

$$E_s = (F_{p_t})(l) \text{ ft-lb} = (1.83 \times 10^{-2})(p_c)(2.0 \text{ ft}) \qquad (4.12)$$

or

$$E_s = 3.65 \times 10^{-2} \, p_c \text{ ft-lbf} \qquad (4.13)$$

The total energy E_t acting upon the projectile would be:

$$E_t = E_d + E_s = (1.02p_c + 3.65 \times 10^{-2} \, p_c) \text{ ft-lbf} \qquad (4.14)$$

or

$$E_t \approx 1.06 \, p_c \text{ ft-lb} \qquad (4.15)$$

The total mass accelerated down the barrel m_{total} is:

$$m_{total} = m_{\substack{accelerated \\ gas}} + m_{projectile} \qquad (4.16)$$

If the projectile mass is assumed to be 6.852×10^{-5} slugs (1 gram) (the approximate mass of .22 caliber pellet):

$$m_{total} = [(2.49 \times 10^{-7})(p_c) + 6.852 \times 10^{-5}] \text{ slugs} \qquad (4.17)$$

If friction and other losses in the system are neglected, the approximate muzzle velocity v_{muzzle} for any value of p_c greater than 30.1 psi (207.7 kPa) can be determined from E_{total} and m_{total} where:

$$v_{muzzle} = \left[2 \left(\frac{E_{total}}{m_{total}} \right) \right]^{\frac{1}{2}} \qquad (4.18)$$

or

46

$$v_{muzzle} = \left[2 \left(\frac{1.06 p_c \, ft - lb}{(2.49 \times 10^{-7} p_c + 6.852 \times 10^{-5}) slugs} \right) \right]^{\frac{1}{2}} \frac{ft}{s} \qquad (4.19)$$

For a sample value of $p_c = 600$ psi (4.14 MPa):

$$v_{muzzle} = 2416 \frac{ft}{s} \left(738 \frac{m}{s} \right) \qquad (4.20)$$

A plot of the predicted performance of the experimental gun based on Equation 4.19 is shown in Figure 4.4.
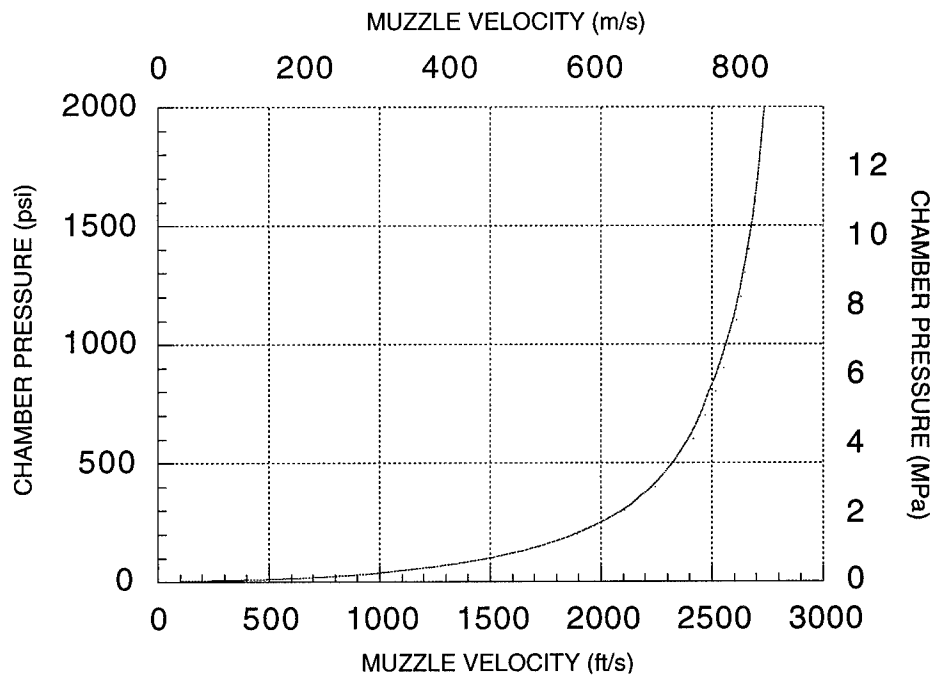
Figure 4.4: Estimated Chamber Pressure versus Muzzle Velocity for Experimental Light-Gas Pellet Gun

While it was understood that because of friction and other unknown losses the actual performance of the gun would fall short of these expectations, the predicted performance was promising and far superior to any commercially available pellet gun.

4.1.2 THE TARGET CHAMBER AND CATCH TANK

A section of steel cylinder was chosen as the catch tank because it could also serve as a curved form for the target surface, a thin sheet of guider material to be attached to the inside of the cylinder. A roughly rectangular hole approximately 15.0 cm x 20.0 cm (6.0 in x 8.0 in) cut in the side of the cylinder section provided the means to shoot at and nearly tangent to the target surface, as shown in Figure 4.5.
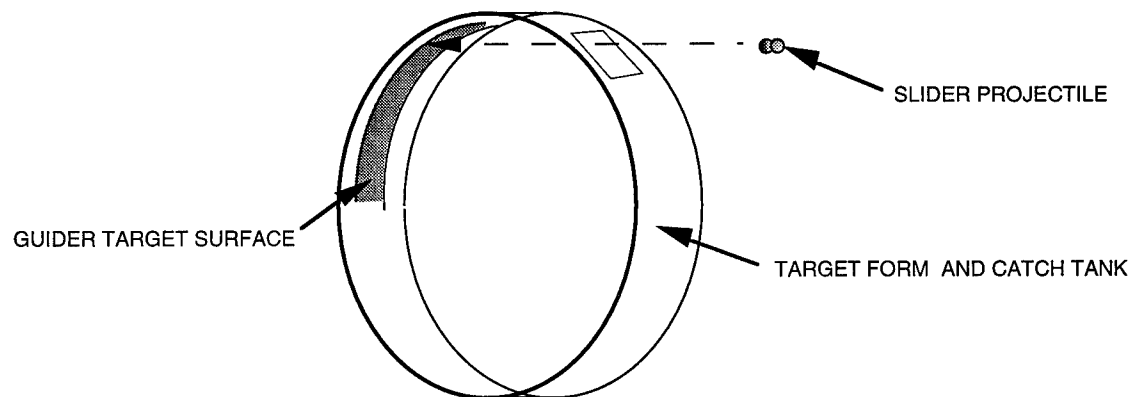
Figure 4.5: Target Form and Catch Tank Concept

The cylinder section was 25.4 cm (10.0 in) wide and 2.54 cm (1.0 in) thick with an inner diameter of 86.36 cm (34.0 in). This particular size of cylinder section was selected from on-hand materials available because it provided a radius of curvature less than that which was used at Ohio State University when gouges were successfully produced (approximately 61 cm (24 in)) [4,23], guaranteeing a greater amount of slider normal force at the same relative sliding velocities. Six to eight shots (iterations of the experiment) could be conducted with each strip of target surface material by carefully aligning the gun and using a strip as wide as the 15.0 cm (6.0 in) hole. The cylinder was positioned standing on its side so that the edge of the guider surface, and ideally the point of slider impact, was on the "top" of the cylinder (see Figure 4.4); the "top" was located using a plum bob and a level. Sawdust placed in the bottom of the cylinder was used to decelerate and catch the slider. Sheets of 1.27 cm (0.5 in) plywood bolted together against the sides of the cylinder formed the remainder of the catch tank enclosure. The actual target cylinder is shown in Figure 4.6.
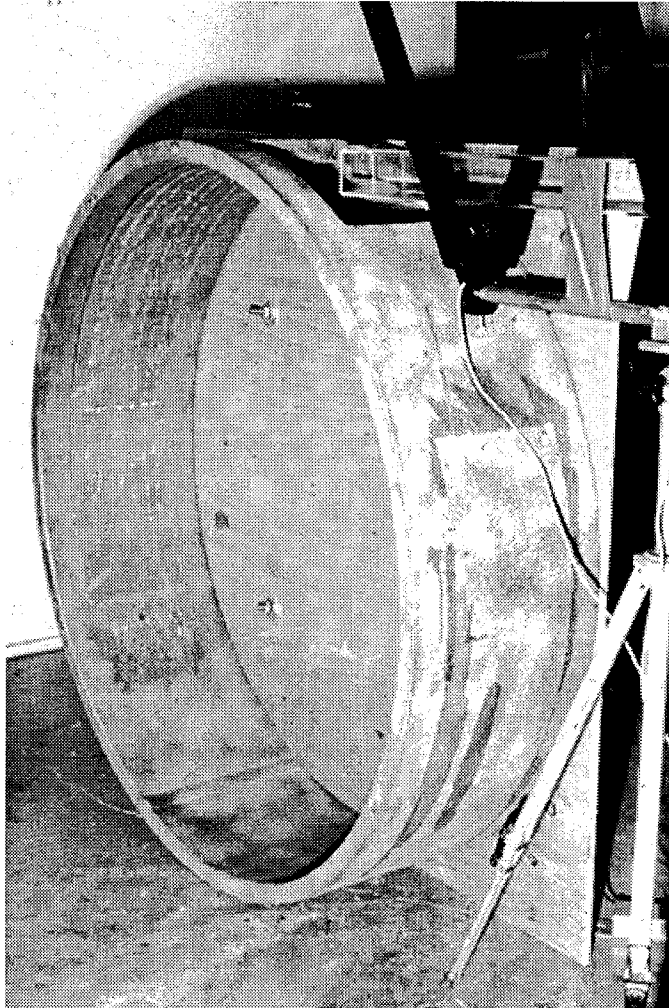
Figure 4.6: Actual Target Cylinder and Catch Tank with Used Guider Surface Attached

4.1.3 DETERMINING THE SLIDING VELOCITY

Over short distances, the effect of aerodynamic drag and the resulting deceleration of a .22 projectile in flight is negligibly small. Accordingly, if the distance of travel in air of a slider fired by a gun is relatively short, the initial sliding velocity is essentially the projectile's muzzle velocity. Similarly, if slider-guider contact is almost tangent and the distance traveled by a slider is relatively short, it can be assumed that the slider velocity at any point along the guider is at best nearly the same as and at worst marginally less than the initial sliding velocity. This is supported by the fact that in the Ohio State experiments, velocity measurements indicated negligible slowing of a projectile by time it reached the end of the curved target [23]. Accordingly, for the purposes of this experiment it was assumed that the in-flight projectile velocity was the same as the slider velocity at any location along the guider.

Frequently with laboratory experiments involving high-velocity guns, "break screens" are used to determine projectile velocity. Break screens are thin, parallel, conducting (usually foil) sheets with current flowing though them that are placed a known distance apart. When a projectile penetrates the screens, electrical impulses are generated that can be read on an oscilloscope and used to determine the projectiles' velocity. Obviously and unfortunately though, a set of break screens must be replaced after every shot. To avoid that problem and simplify this experiment, it seemed more practical to use a ballistic chronograph instead to determine projectile and thus initial sliding velocity. A ballistic chronograph is a self-contained device commonly used by expert marksmen and small arms ammunition

51

manufacturers to determine bullet velocities and thus statistical variations in and between lots of ammunition. Accordingly, a Model 35 Proof ballistic chronograph was purchased from Oehler Research of Austin, Texas.

The Oehler Model 35 Proof chronograph, shown in Figure 4.7, consists of series of optical sensors that "see" the shadow created by a projectile passing between a diffused light source and the sensor. The sensors are positioned a known distance apart on a mounting rod which is then attached to an ordinary camera tripod. A microprocessor calculates the velocity of a projectile fired over the sensors and displays the velocity in ft/s or m/s, depending on the fixed distance between the sensors. In this experiment, velocities were measured in ft/s and then converted to m/s. The microprocessor of the Model 35 Proof chronograph is powered by one 9 volt battery; the lights for the sensors, which are not needed when the chronograph is used outdoors, require a 110/120 volt power source.
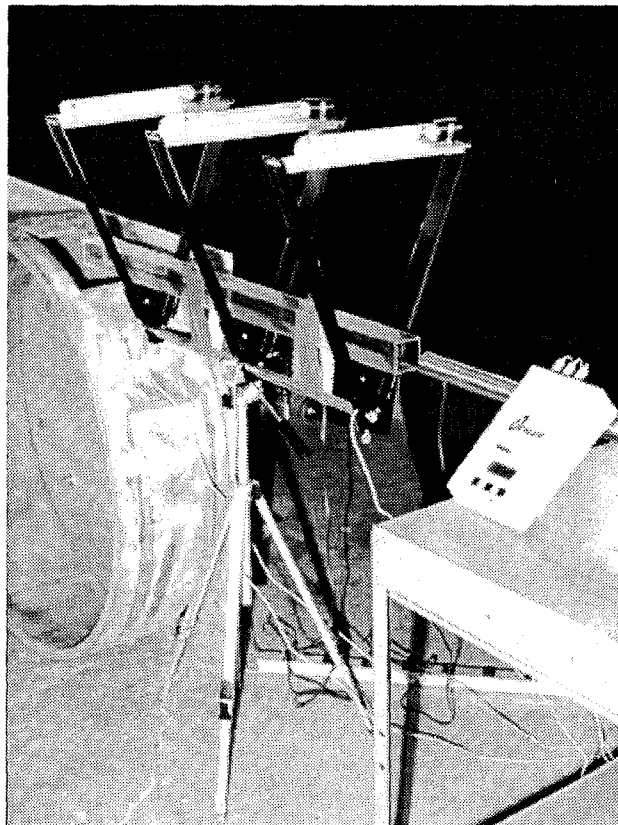
Figure 4.7: The Oehler Model 35 Proof Chronograph,

4.1.4 DETERMINING THE ANGLE OF INCIDENCE

For the target configuration in this experiment, the angle of incidence of the slider projectile can be determined with simple geometry, as shown in Figure 4.8.
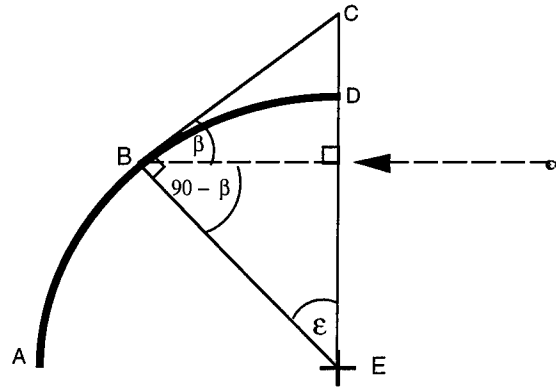
Figure 4.8: Geometry of Slider Impact on Inner Surface of Catch Tank

Arc A-D reflects a portion of the catch tank where point D is the start of the guider surface and is perfectly horizontal with the ground. If a slider-projectile traveling horizontally strikes arc A-D at point B, the radius to point B is line segment B-E, the tangent to point B is line segment B-C, and by similar triangles angle β is equal to angle ε. Angle ε can be determined from:

$$\varepsilon = \frac{2\pi r(360^0)}{arc_{B-D}}$$

(4.21)

where: r = cylinder inner radius = length of line segment B-E

arc_{B-D} = measured distance from edge of guider surface to point of slider impact

In this way, Equation 4.21 was used to determine the angle of slider incidence. Values of the angle of incidence for all of the iterations of the experiment are tabulated in Table 5.1

4.1.5 DETERMINING THE SLIDER NORMAL FORCE AND CONTACT STRESS

Calculating the normal force generated by a slider on a curved surface is easily accomplished. It is well known that:

$$a_n = \frac{v_t^2}{r} \qquad (4.22)$$

where: a_n = normal acceleration

v_t = tangential velocity

r = radius of curvature

and

$$F = ma \qquad (4.23)$$

where: F = force

m = mass

a = acceleration

With the assumptions that the velocity measured by the chronograph is the same as the sliding velocity at any point on the slider and that the slider mass at any point is the average of the initial and final masses, the average normal force generated by the slider is:

$$F_{\substack{slider}} = m_{\substack{projectile \\ (average)}} \frac{v^2_{\substack{measured}}}{r_{\substack{target \\ cylinder}}} \qquad (4.24)$$

Calculating a realistic value for the slider contact stress is more difficult because the actual contact area between the slider and guider is unknown and difficult to accurately estimate. The method used by Graff et al. [23] calculated contact stress at the slider-guider interface by using the contact area and projectile mass as determined from the width of the sliding wear track as follows. It is known that:

$$\sigma = \frac{F}{A} \qquad (4.25)$$

where: σ = stress

F = force

A = area

Combining Equations 4.24 and 4.25 yields:

$$\sigma_{\substack{contact}} = \frac{m_{\substack{average}} v^2_{\substack{measured}}}{A_{\substack{measured}} r_{\substack{target \\ cylinder}}} \qquad (4.26)$$

56

If it is possible to accurately determine slider mass and contact area from the width of a wear track then, it is possible to determine the slider-guider contact stress in the way that Graff et al. did. It is known, however, that two solid materials placed in contact actually touch each other only at discrete points of contact or "junctions" and that the actual or "real" area of contact A_r is somewhat less than the apparent area of contact A_a [28]. Because the calculations of Graff et al. used a measured value of A_a, they likely overestimated A_r and accordingly underestimated the actual value of contact stress in the Ohio State experiments.

It has been shown that it is possible to calculate a minimum value for A_r that is very close to the actual value of the real area of contact. Though there are circumstances that can alter the relation, the value of A_r, based on the assumption of ideally plastic deformation, is generally [28]:

$$A_r \geq \frac{L}{p} \tag{4.27}$$

where: L = the force (in kilograms) normal to the surfaces in contact
which is pressing them together = $\dfrac{F_{slider}}{g_c}$

p = largest compressive stress that a region of material can carry without plastic yielding, known as the "penetration hardness " (for lead, $p = 4 \ \dfrac{kg}{mm^2}$ [28])

For this experiment, then:

$$A_r \geq \frac{m_{average} v^2_{measured}}{pg_c r_{target \atop cylinder}} \qquad (4.28)$$

where: g_c = gravitational constant = $9.8 \, \frac{m}{s^2}$

With a fairly accurate estimate of the minimum possible slider-guider contact area from Equation 4.27, it is possible to estimate the maximum possible contact stress. For this experiment, it can be said that:

$$\sigma_{contact} = \frac{F_{slider}}{A_r} \qquad (4.29)$$

Combining Equations 4.24, 4.28, and 4.29 yields:

$$\sigma_{contact} \leq \frac{\left(\dfrac{m_{average} v^2_{measured}}{r_{target \atop cylinder}} \right)}{\left(\dfrac{m_{average} v^2_{measured}}{pg_c r_{target \atop cylinder}} \right)} \qquad (4.30)$$

or

$$\sigma_{contact} \leq pg_c \qquad (4.31)$$

58

This unusual result defies intuition and suggests that the maximum contact stress generated by a slider on a curved surface is a function only of the indentation hardness of the material and is not a function of either the sliding velocity or sliding mass. Accordingly, the calculated maximum possible contact stress would be the same for every repetition of the experiment as long as the materials were not changed. This is somewhat confusing.

An alternate method of dealing with the contact stress is to assume that when surface deformations such as gouging occur, the contact stress must at least equal the known yield stress of the material. Given this, it is possible to work backwards and use the calculated normal force from Equation 4.24 to estimate the area of contact, where:

$$A_{estimated} = \frac{\left(\dfrac{m_{projectile} v^2_{measured}}{r_{target \atop cylinder}}\right)}{\sigma_{yield}} \qquad (4.32)$$

4.2 SELECTING SLIDER AND GUIDER MATERIALS

In attempting to create low relative velocity gouges, it was critical to select the correct slider and guider materials. Ideally, these would be materials prone to gouging and with a gouging onset velocity that would fall within the capabilities of the experimental set-up to be used. Based on the plots in Figures 3.1 - 3.3, it was known that the slider at a minimum should be

a metal with a low yield strength and preferably high density as well. It was also known that using materials either on hand or commercially available would minimize expense and experimental set-up time.

4.2.1 THE SLIDER

Lead seemed like a natural choice for the slider for a number of reasons. First and foremost, lead is a low strength, soft material with a density of 11.35 g/cm^3 (0.385 lb/in^3) and an average yield strength of 33.0 MPa (4.8 ksi) [33]. If prone to gouging and in compliance with the graphical relation in Figure 3.3, these properties indicate that a system with a lead slider would experience the onset of gouging at a velocity of approximately 218 m/s (715 ft/s). Further, in the experiments conducted at Ohio State University, lead was found to produce heavy gouges (as were tin, zinc, and 50-50 solder, all materials with a low melting point yet widely varying hardness) though the projectiles tended to break up during acceleration [23]. Finally, .22 caliber lead pellets are readily available in numerous varieties, eliminating the need to manufacture specialized projectiles for the pellet gun. Accordingly, lead in the form of "air rifle" pellets was chosen as the slider material. Specifically, Daisy .22 caliber standard match "wadcutter" pellets, shown in Figure 4.9, were used because they were available in the laboratory.
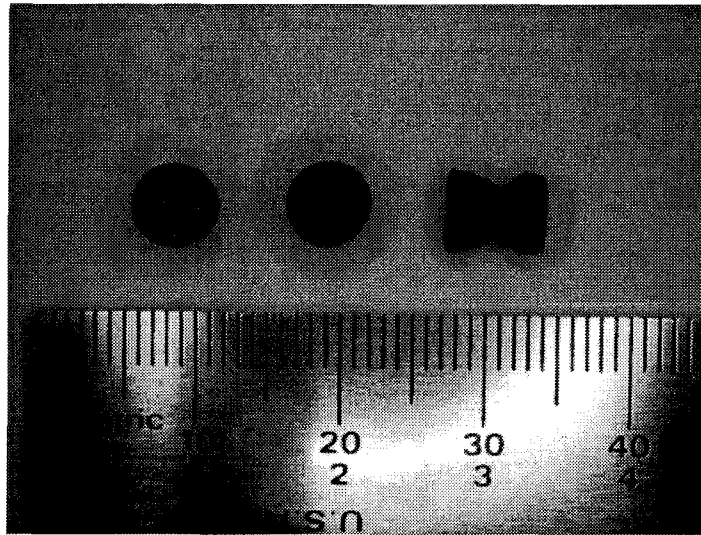
Figure 4.9: Front, Rear, and Side View of Daisy .22 Caliber Standard Match "Wadcutter" Pellets (left to right, respectively)

4.2.2 THE GUIDER SURFACE

In many of the instances of gouging reported, the slider and guider were either identical or similar materials. For this reason and those that influenced the selection of lead as the slider material, lead also seemed like an appropriate choice for the guider material even though gouging of lead surfaces had never before been reported. As lead sheet is commercially available in a variety of sizes and thicknesses, it was chosen as the guider material.

Two sheets of 91.0 x 91.0 cm (36.0 x 36.0 in) lead sheet were purchased from Lead Products Co., Inc. of Houston, Texas. Two different thicknesses, 3.18 mm (0.125 in) and 6.35 mm (0.25 in), were selected so that the effect of

61

guider thickness upon gouging, if any occurred, could be observed. From these sheets, 15.0 x 91.0 cm (6.0 x 36.0 in) guider strips were cut with tin snips. After were flattening them by rolling the target cylinder over them, these strips were attached to the inner surface of the target cylinder with 3M Super Trim Spray Adhesive by using a smaller steel cylinder as a roller. After being used, these strips were removed from the target cylinder with acetone and a putty knife.

4.3 EXPERIMENTAL PROCEDURE

A cycle of experimentation would required the following steps. This entire procedure, excluding the attachment of guider surface to the target cylinder, would take 30 - 40 minutes to complete.

A strip of guider material was cut and attached to the inner surface of the steel target cylinder. The cylinder was positioned with the window and forward edge of the guider surface on "top" (as discussed in Section 4.1.2) and held in place with a wooden door stop.

The chronograph was positioned using a 5.08 cm (2.0 in) square, 91.0 cm (36.0 in) long, clear, acrylic tube with 3.18 mm (0.125 in) thick sides placed over the sensors of the chronograph and taped to the sensor's mounting rod to serve as the projectile flight tube. The chronograph tripod assembly was situated such that the end of the acrylic tube would protrude into the interior of the target cylinder through the hole cut in the side.

The gun was then loaded as follows. A pellet was selected and weighed to determine the initial mass. Once weighed, it was lightly coated

with Hoppe's Gun Oil and tapped into breach end of the helium gun barrel using a section of barrel cleaning rod. A rupture diaphragm was cut from a sheet of mylar and stuck with vacuum grease to an o-ring over the opening on the forward end of the pressure chamber. The barrel assembly was then closed against and bolted to the pressure chamber "breech".

After loading the gun, the cart on which it rested was positioned so that the gun would fire through the acrylic tube attached to the chronograph and so that the muzzle of the gun was slightly inside the acrylic tube. The gun was "leveled" by placing a level on the barrel and shims under the breech so that sliders would be fired parallel to the ground and nearly tangent to the forward edge of the guider surface at the top of the target cylinder. A piece of string running from the breech of the gun to the top of the target cylinder was used to align the barrel with the desired point of impact on the guider surface. Using the string as a visual guide, the gun was repositioned as required so that the string was parallel to the sides of the target cylinder and, from behind the target cylinder, appeared to bisect the width of the gun barrel. After this had been done, the level of the barrel was verified. Once this was completed, the gun had been aligned to fire the slider straight and level at the guider surface.

After the aligning the gun, the plywood sides of the catch tank were placed against the sides of the target cylinder and bolted together through the interior of the cylinder using four pieces of 6.35 mm (0.25 in) diameter, 33 cm (13 in) long "all-thread." An additional small piece of plywood was placed over the hole in the target cylinder to prevent debris, and the pellet in the event that it traversed a complete loop, from flying out of the cylinder. The

63

chronograph and its lights were then turned on in the event that the mylar diaphragm ruptured during chamber pressurization, allowing the gun to fire prematurely. When this was complete, the gun chamber was pressurized by opening the regulator valve on the helium cylinder. When the desired chamber pressure was reached, as determined by reading the pressure gauge on the assembly attached to the chamber, the regulator valve on the helium cylinder was closed.

The gun was then fired by closing an electric switch. After firing, the projectile velocity was immediately recorded from the chronograph. The sides of the target cylinder were then removed and the fired pellet recovered from the sawdust in the cylinder. The final mass of the pellet was determined by weighing the pellet again on a scale.

CHAPTER 5

EXPERIMENTAL RESULTS

The experiment proved resoundingly successful in accomplishing all of the stated objectives. The conditions of sliding contact as well as gouges were created and, as precisely as possible, the gouging onset velocity of lead sliding on lead was identified. With each shot being one iteration of the experiment, a total of twenty-five shots were conducted with initial sliding velocities ranging from 150 to 482 m/s (493 to 1580 ft/s). Four of these hit the edge of the lead guider surface and were of no experimental value. All of the remaining twenty-one shots marked the length of the guider-target surface with a wear track indicating the path followed by the slider. Sixteen of these shots produced at least one incipient gouge, the slowest having an initial sliding velocity of 245 m/s (804 ft/s). All shots with initial sliding velocities above 274 m/s (900 ft/s) consistently produced gouging. All of shots with initial sliding velocities above 305 m/s (1000 ft/s) produced moderate to severe gouging.

5.1 EXPERIMENTAL DATA

5.1.1 TABULATED DATA

As discussed in Chapter 4, data for each iteration of the experiment was either measured directly or calculated. Reflected in Table 5.1 is data from the twenty-five shots conducted. The calculated maximum average contact

stress $\sigma_{contact}$ from Equation 4.29 was 39.20 N/mm^2 (5,684 psi) for every shot. Because this figure is somewhat confusing, the real area of contact A_r was used as a means to check its validity. It was felt that if the estimated values of A_r as determined by equations 4.28 and 4.32 were fairly close, this would be indicative of the accuracy of the calculated value of $\sigma_{contact}$, which requires input from Equation 4.28. As can be seen in Table 5.1, the two methods of calculating A_r provide surprisingly similar results, suggesting that Equation 4.29 is a valid means of determining the maximum contact force generated by a slider on a curved surface.

S H O T #	GUN HELIUM CHAMBER PRESSURE [kPa (psi)]	ANGLE OF INCID. (deg.)	INITIAL SLIDING VELOCITY [m/s (ft/s)]	SLIDER MASS (g)			SLIDER NORMAL FORCE [N (lbf)]	CONTACT AREA FROM EQUATION 4.28 [mm^2(in^2)]	CONTACT AREA FROM EQUATION 4.32 [mm^2(in^2)]	GOUGES ?
				INITIAL	FINAL	CHANGE				
1	4690 (680)	6	≈320 (1050)	Unknown	Unknown	Unknown	246 (55)	7.46 (0.0116)	6.27 (0.0097)	YES
2	2069 (300)	13	150 (493)	1.0392	1.0358	- 0.0034	54 (12)	1.64 (0.0025)	1.38 (0.0021)	NO
3	2759 (400)	15	218 (715)	1.0216	1.0033	- 0.0183	111 (25)	3.37 (0.0052)	2.84 (0.0044)	NO
4	3448 (500)	12	262 (867)	1.0245	0.9919	- 0.0326	163 (36)	4.94 (0.0077)	4.15 (0.0064)	YES 1 Incipient
5	4138 (600)	8	297 (980)	1.0381			107 (24)	3.25 (0.0050)	2.73 (0.0042)	YES
6	3448 (500)	6	279 (914)	1.0375	0.9690	- 0.0685	180 (40)	5.46 (0.0085)	4.59 (0.0071)	YES
7	3241 (470)	-	Hit Edge	1..0323	Broke Up	Unknown				NO
8	3310 (480)	-	Hit Edge	1.0240	Broke Up	Unknown				NO
9	3310 (480)	9	258 (847)	1.0282	0.9718	- 0.0564	154 (34)	4.68 (0.0072)	3.93 (0.0061)	YES Incipient at Scratches
10	3172 (460)	10	250 (821)	1.0273	0.9877	-0.0396	146 (33)	4.43 (0.006)9	3.72 (0.0058)	NO
11	3379 (490)	15	262 (858)	1.0244	0.7341	-0.2903	139 (31)	4.22 (0.0065)	3.55 (0.0055)	NO
12	3517 (510)	12	273 (895)	1.0366	0.7667	-0.2699	155 (35)	4.71 (0.0073)	3.96 (0.0061)	YES 2 Incipient
13	3586 (520)	5	290 (953)	1.0366	0.9739	-0.0627	196 (44)	5.95 (0.0092)	5.01 (0.0078)	YES
14	2552 (370)	9	245 (804)	1.0241	0.9817	-0.0424	139 (31)	4.23 (0.0066)	3.55 (0.0055)	YES 1 Incipient
15	2897 (420)	4	263 (863)	1.0321	0.9855	-0.0466	162 (36)	4.90 (0.0076)	4.12 (0.0064)	YES
16	3103 (450)	-	Hit Edge	1.0311	0.5964	-0.4347				NO
17	3103 (450)	4	277 (909)	1.0247	0.9525	-0.0722	176 (39)	5.33 (0.0083)	4.48 (0.0069)	YES
18	3379 (490)	-	Hit Edge	1.0200	0.0461	-0.9739				YES
19	3310 (480)	4	279 (915)	1.0385	0.9767	-0.0618	181 (41)	5.50 (0.0085)	4.62 (0.0072)	YES
20	4138 (600)	8	315 (1033)	1.0922	0.9352	-0.157	233 (52)	7.05 (0.0109)	5.93 (0.0092)	YES
21	4897 (710)	4	282 (924)	1.0838	0.9944	-0.0894	191 (43)	5.78 (0.0090)	4.86 (0.0075)	YES
22	6207 (900)	3	355 (1165)	1.0935	0.7863	-0.3072	274 (61)	8.32 (0.0129)	6.99 (0.0108)	YES
23	7793 (1130)	3	397 (1303)	1.0896	0.6174	-0.4722	312 (70)	9.45 (0.0146)	7.94 (0.0123)	YES
24	8552 (1240)	5	429 (1406)	1.0829	0.6826 (Broke Up)	-0.4003	375 (84)	11.38 (0.0176)	9.57 (0.0148)	YES Severe
25	11931 (1730)	3	482 (1580)	1.0922	0.6212 (Broke Up)	-0.5952	460 (103)	13.94 (0.0216)	11.73 (0.0182)	YES Severe

Table 5.1: Tabulated Experimental Data

5.1.2 GUN PERFORMANCE CURVE

As the experiment progressed, actual chamber pressure and projectile velocity data were contrasted by plotting and generating a fitted gun performance curve. With this curve, as more data was generated it was possible to use the curve fit with increasing accuracy to predict the projectile muzzle velocity and thus choose an initial sliding speed for an iteration of the experiment. The final gun performance curve is shown in Figure 5.1.
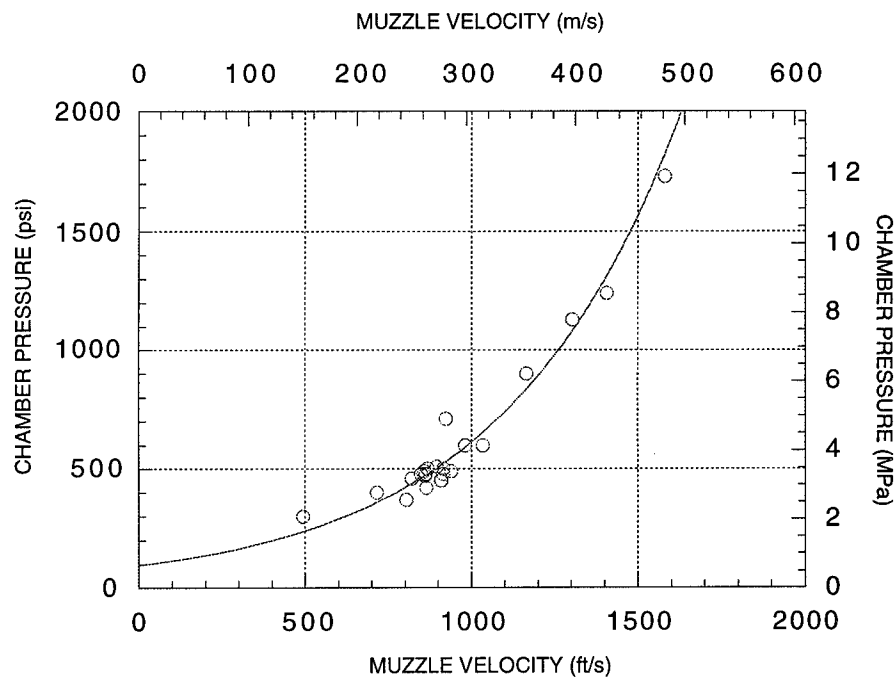
Equation of Curve Fit: $y = -2423.9 + 1228.2\log(x)$ (R = 0.96)

Figure 5.1: Chamber Pressure versus Muzzle Velocity for Experimental .22 Caliber Light-Gas Pellet Gun

5.2 DESCRIPTION OF FINDINGS

All shots creating the desired effect of nearly tangential slider-guider impact and a subsequent sliding interface resulted in the length of the guider surface being marked with a wear track indicating the path of travel followed by the slider. Variations in the slider angle of incidence and initial sliding speed produced corresponding changes in the appearance of the track. Gouges, when present, began within the width and were randomly placed along the length of the track. In all Figures showing wear tracks or gouges, slider relative motion was from left to right.

5.2.1 INITIAL CONTACT REGION

Both slider angle of incidence and initial velocity affected the appearance of the initial contact region or impact "fan". The greater the angle of incidence, the shorter and more sharply angled the impact fan was, as indicated in Figure 5.2.
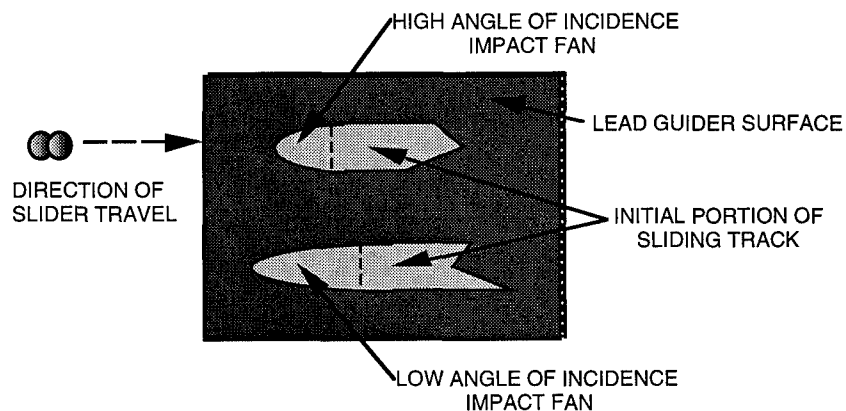
Figure 5.2: Sketch of Slider Impact Fans and Initial Portion of Sliding Tracks

69

Increasing the slider initial velocity and the corresponding slider normal force caused far more dramatic changes in the impact fan than did variations in the angle of incidence. At the lowest initial sliding speed achieved of 150 m/s (493 ft/s), the impact fan was primarily an indentation in the lead guider surface with little removal of the oxide layer and only minor wear evident, as can be seen in Figure 5.3.
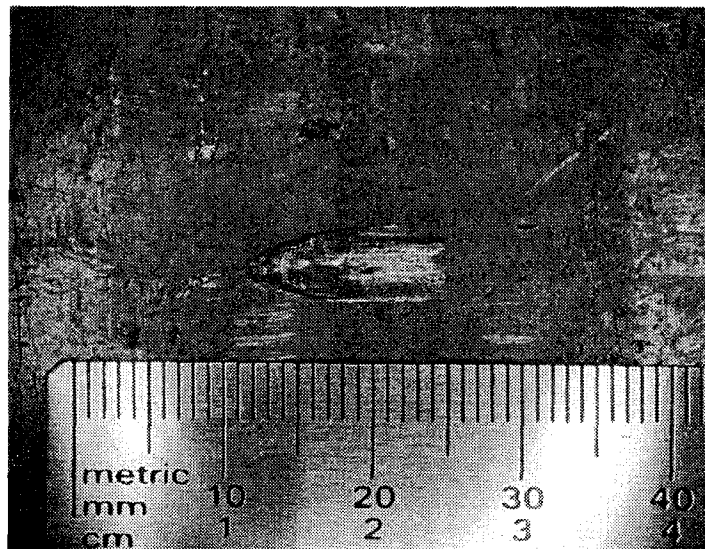
Figure 5.3: Impact Fan Produced at 150 m/s (493 ft/s) on 3.18 mm (0.125 in) Thick Lead Sheet

Beginning at 218 m/s (715 ft/s), the impact fan consisted of multiple, overlapping craters or "dimples," elongated in the direction of slider travel. Shaped like gouges and having a raised lip, these indentations were distinguishable by their shiny, bright, silvery finish and had striations in the direction of slider travel. These shiny gouges can be seen in Figure 5.4.
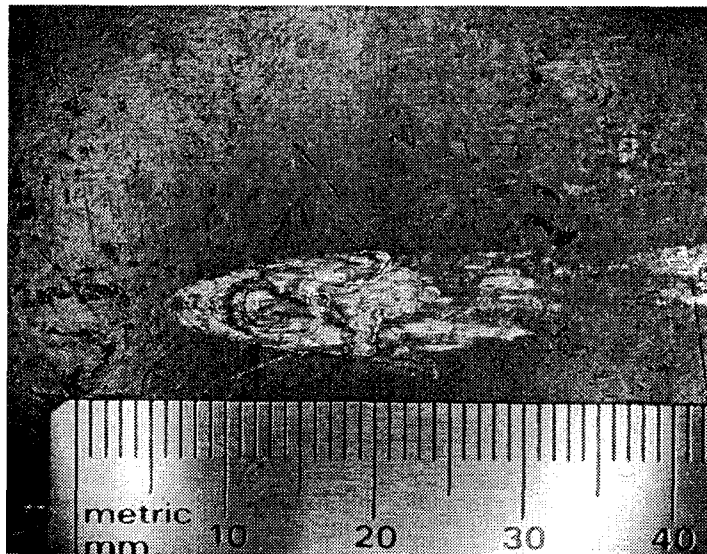
Figure 5.4: Impact Fan Produced at 264 m/s (867 ft/s) on 3.18 mm (0.125 in) Thick Lead Sheet

Beginning at 273 m/s (895 ft/s), interspersed with the shiny gouges were others with the dull finish and raised lip normally associated with gouging. Often though, these were reminiscent of "splashes," having a more smooth and melted appearing surface texture than on gouges appearing further downstream on the same sliding track or on other sliding tracks generated at similar relative sliding velocities. An example of these "splash" gouges can be seen in Figure 5.5.
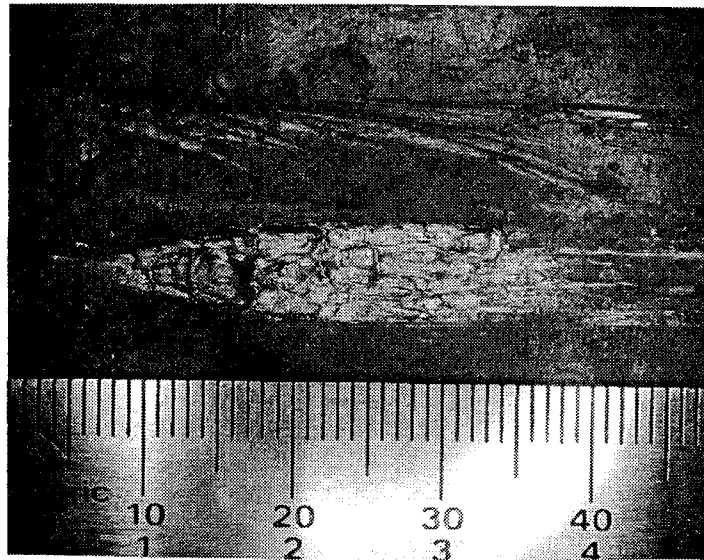
Figure 5.5: Impact Fan Produced at 299 m/s (980 ft/s) on 3.18 mm (0.125 in)
Thick Lead Sheet

As initial sliding speed increased, the number of shiny gouges diminished while the number of dull, smooth gouges increased. At 315 m/s (1033 ft/s), only one large crater in the fan had a shiny finish, as shown in Figure 5.6. Again, all of the other overlapping indentations appeared to be characteristic gouges but with a more smooth and melted appearing surface texture.
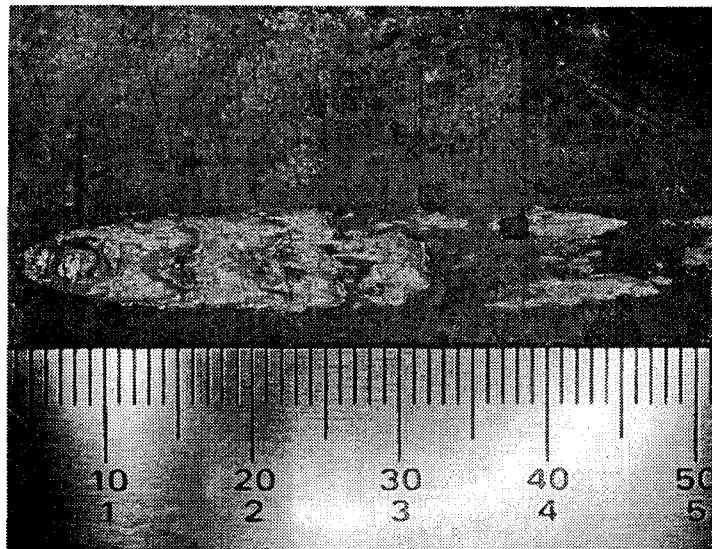
Figure 5.6: Impact Fan Produced at 315 m/s (1033 ft/s) on 3.18 mm (0.125 in) Thick Lead Sheet

At 355 m/s (1165 ft/s) and above, only dull smooth gouges were present in the impact fan, as can be seen in Figure 5.7 (and in Figures 5.8, 5.17, and 5.22 as well).
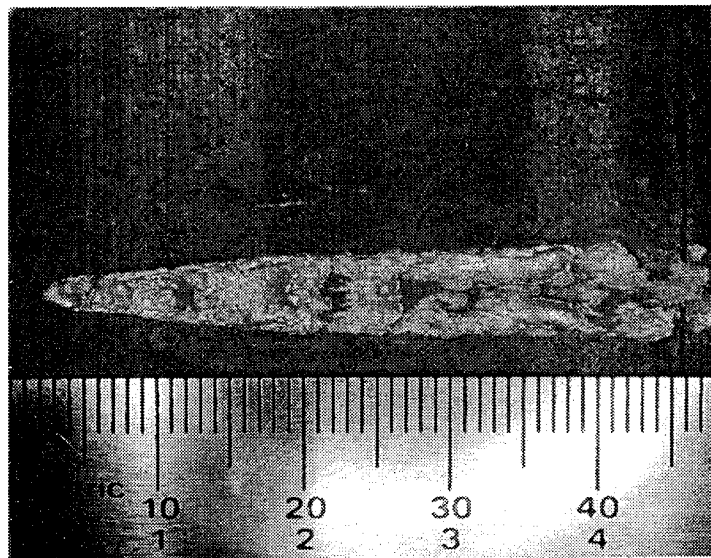
Figure 5.7: Impact Fan Produced at 355 m/s (1165 ft/s) on 3.18 mm (0.125 in) Thick Lead Sheet

At 397 m/s (1303 ft/s) and above, these dull impact fan gouges appeared progressively more like splashes, as can be seen in Figure 5.8. They continued to have a smooth interior surface finish and had a distinctly raised lip around the forward half to two-thirds of circumference of the gouge as well.

Figure 5.8: Impact Fan Produced at 397 m/s (1303 ft/s) on 3.18 mm (0.125 in) Thick Lead Sheet

Above 397 m/s (1303 ft/s) the largest of theses gouges grew continually longer and deeper but their appearance was otherwise unchanged.

5.2.2 SLIDING TRACKS

As in the Ohio State experiments, the sliding wear tracks in this experiment were characterized by a region indicating the initial impact and flattening of the slider followed by a straight, easily identifiable wear track along the remainder of the length of the guider surface [4,23]. From observation alone, it is uncertain whether the sliding tracks resulted from removal of the guider surface oxide layer, the transfer of slider wear particles, or the deposition of melted surface layer material from the slider which is known to exist at high velocities [25,26]. However, as all sliders lost mass during sliding (as indicated by before and after measurements) and because gouging, where present, occurs primarily in the guider surface (it is postulated to occur simultaneously in the slider surface), all of these mechanisms are likely involved.

At initial sliding velocities up to 258 m/s (847 ft/s), the appearance of the portion of the sliding track immediately following the impact fan was fairly uniform and indicated contact between the slider and guider across the full width of the deformed slider for a distance greater than the length of the slider, as can be seen in Figure 5.9.
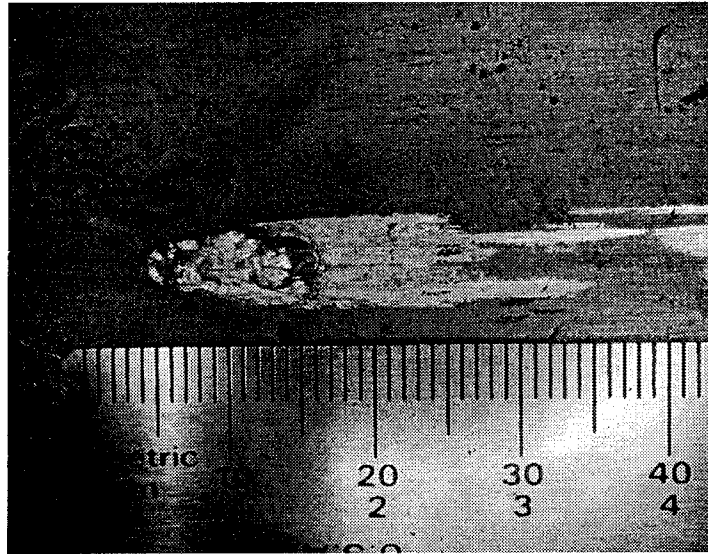
Figure 5.9: Impact Fan Produced at 258 m/s (847 ft/s) on 6.35 mm (0.25 in) Thick Lead Sheet

Beyond this region though, in virtually all iterations of the experiment with initial sliding velocities faster than 258 m/s (847 ft/s), there were indications of intermittent slider-guider contact along portions of, if not the entire wear track. Where slider-guider contact was intermittent, the wear tracks suggested cyclic skipping and/or side-to-side oscillation (balloting) of the slider, as shown in Figures 5.10 and 5.11.
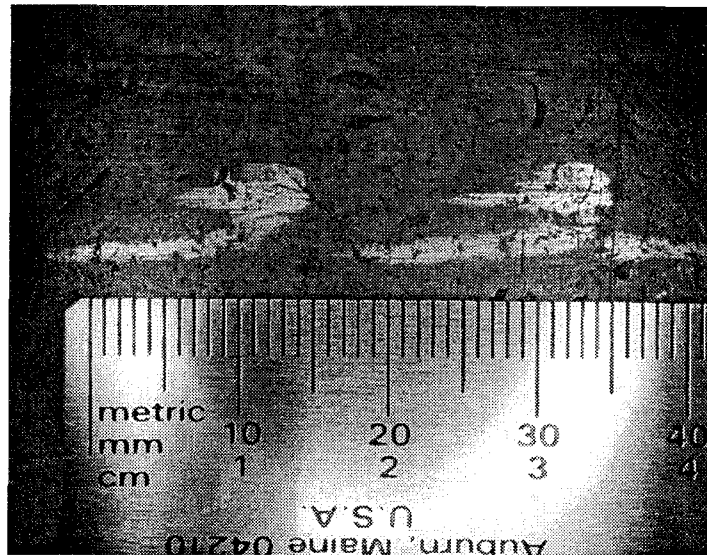
Figure 5.10: Wear Track Produced by Oscillating and Skipping Slider at
279 m/s (914 ft/s) on 6.35 mm (0.25 in) Thick Lead Sheet
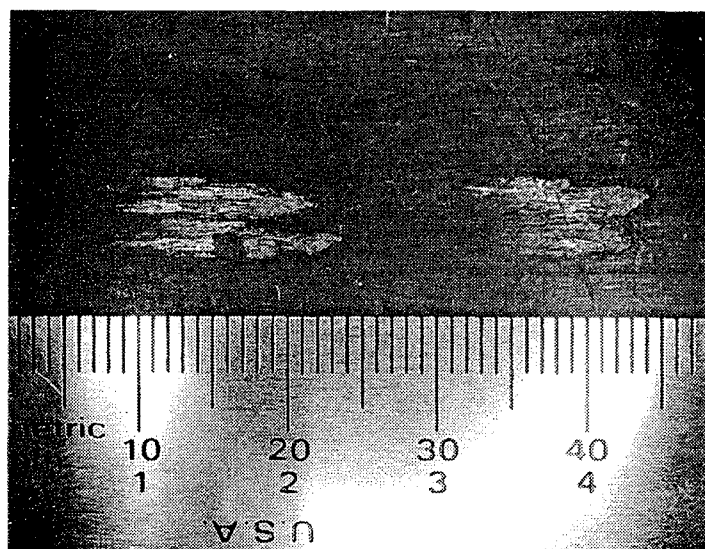
Figure 5.11: Wear Track and Gouges Produced by Skipping Slider at 279 m/s
(915 ft/s) on 3.18 mm (0.125 in) Thick Lead Sheet

It is also interesting to note that these contact regions often exhibited the characteristic teardrop shape of gouges regardless if gouging was present. This was true even at 150 m/s (493 ft/s), the lowest initial sliding speed achieved and well below the apparent gouging threshold for lead (discussed in section 5.2.4), as shown in Figure 5.12.
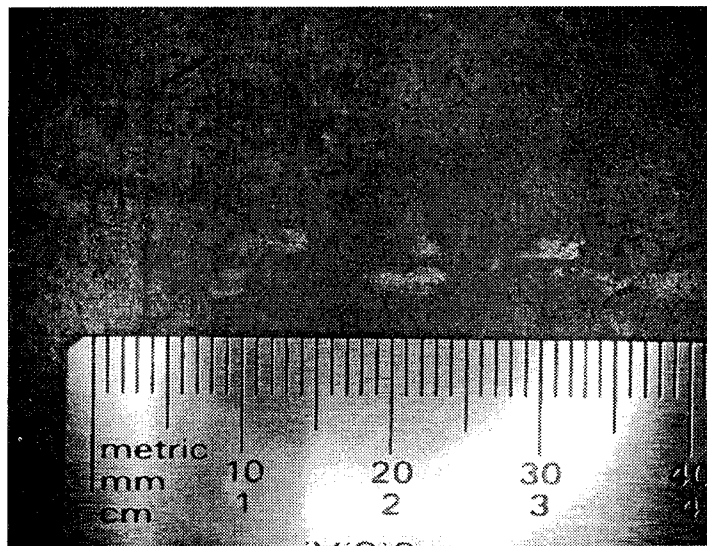
Figure 5.12: Slider-Guider Contact Regions at 150 m/s (493 ft/s) on 3.18 mm
(0.125 in) Thick Lead Sheet

These unique wear patterns clearly did not result from slider tumbling or rotation. In all iterations of the experiment except the last two (during which the sliders broke up), the recovered sliders had a flattened, worn surface where sliding contact had taken place while the opposite side exhibited the crumpled but otherwise unaltered and still recognizable characteristics of an original .22 caliber pellet (as discussed in Section 5.2.4).

Another unique wear pattern observed in some of the sliding tracks suggested periods of contact slider-guider contact either mostly or only at the side edges of the slider. The result, likely due to the fact that the .22 caliber pellets used are essentially hollow, appeared similar to "railroad rails," as shown in Figure 5.13.
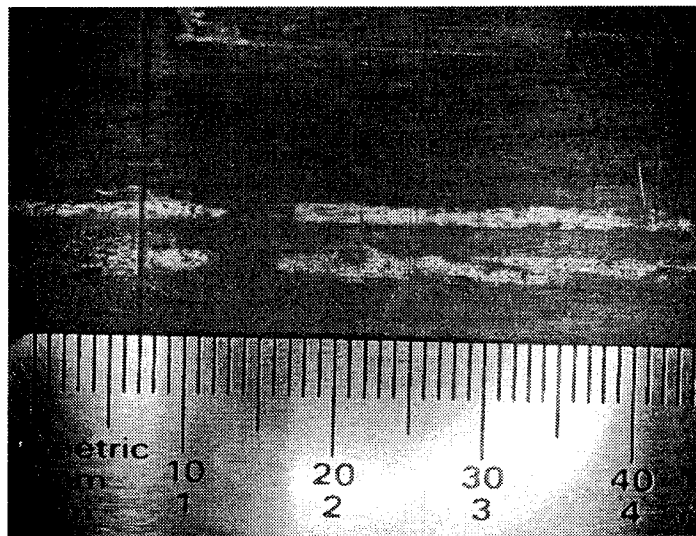
Figure 5.13: "Railroad" Wear Track Produced at 277 m/s (909 ft/s) on
3.18 mm (0.125 in) Thick Lead Sheet

Beyond the impact fan, the sliding track gradually increased in width over the length of the guider, indicating that deformation and flattening of the slider was a continual process. This was progressively more evident on sliding tracks produced with increasing initial sliding velocities up to 397 m/s (1303 ft/s), beyond which the sliders broke up apparently after sliding a short distance.

80

5.2.3 GOUGING

Gouging downstream of the impact fan occurred consistently in shots with initial sliding velocities above approximately 272 m/s (900 ft/s). All shots with initial sliding velocities above 305 m/s (1000 ft/s) produced moderate to severe gouging. Though the gouges produced varied in shape and size, virtually all of them were either tear-drop, "peanut," or oval shaped, as sketched in Figure 5.14.

TEAR-DROP   PEANUT   OVAL

DIRECTION OF SLIDER TRAVEL
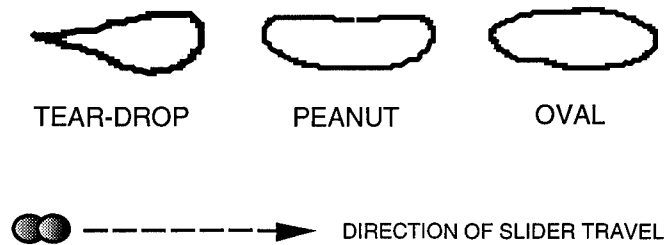
Figure 5.14: Typical Gouge Shapes

While small gouges were observed at all sliding speeds above the gouging threshold velocity, the largest gouges produced occurred at the highest initial sliding velocity achieved.

Regardless of shape and size, all gouges produced had the dull finish, rough or scraped appearance, and raised lip normally associated with gouging. Some of these characteristic gouges produced are shown in Figures 5.15 and 5.16.
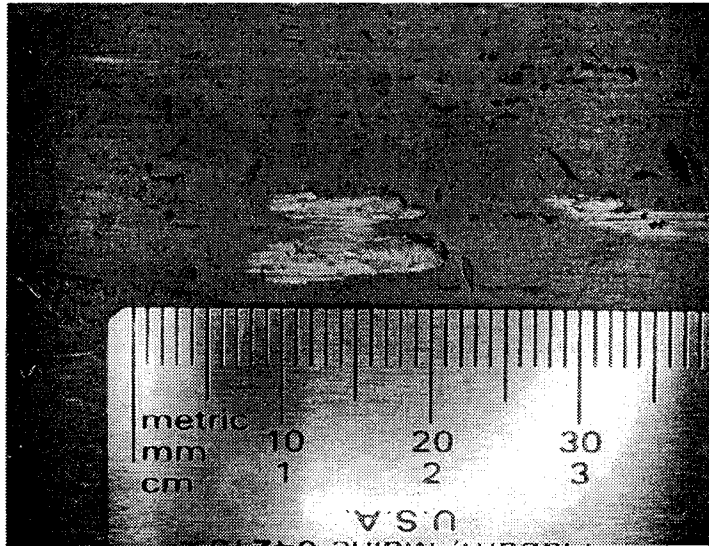
Figure 5.15: Gouges Produced at 290 m/s (953 ft/s) on 6.35 mm (0.25 in) Thick Lead Sheet
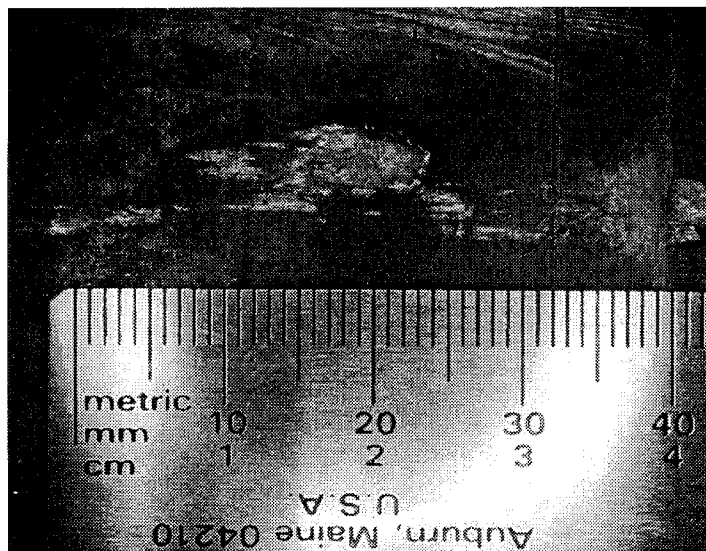
Figure 5.16: Gouge Produced at 299 m/s (980 ft/s) on 3.18 mm (0.125 in) Thick Lead Sheet

Interestingly though, with increasing initial sliding velocity, gouges produced downstream appeared progressively more like the impact fan "splash" gouges described in Section 5.2.1. At 482 m/s (1580 ft/s), the lone impact fan "splash" gouge and downstream gouges are identical as can be seen in Figure 5.17.

Figure 5.17: Impact Fan and Gouges Produced at 482 m/s (1580 ft/s) on 3.18 mm (0.125 in) Thick Lead Sheet

The proportion of gouges to contact wear scars without gouges also increased with initial sliding velocity. In both cases, this continued to the point that at 482 m/s (1580 ft/s), the fastest shot conducted, the wear track was comprised only of numerous "splash" gouges of various sizes, as can also been observed in Figure 5.17. More examples of downstream "splash" gouging are shown in Figures 5.18 - 5.20.
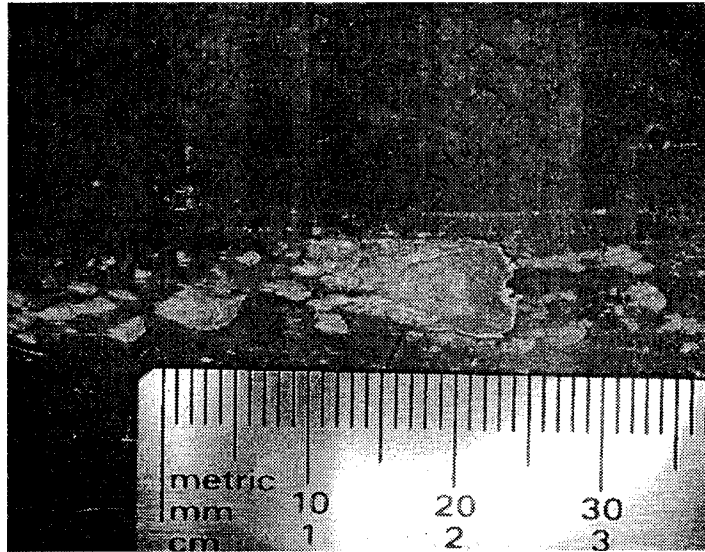
Figure 5.18: "Splash" Gouges Produced at 397 m/s (1303 ft/s) on 3.18 mm (0.125 in) Thick Lead Sheet
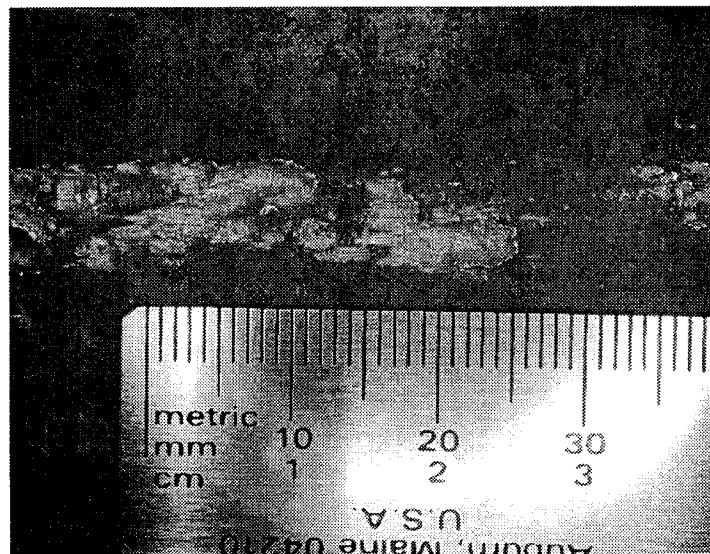
Figure 5.19: "Splash" Gouges Produced at 429 m/s (1406 ft/s) on 3.18 mm (0.125 in) Thick Lead Sheet
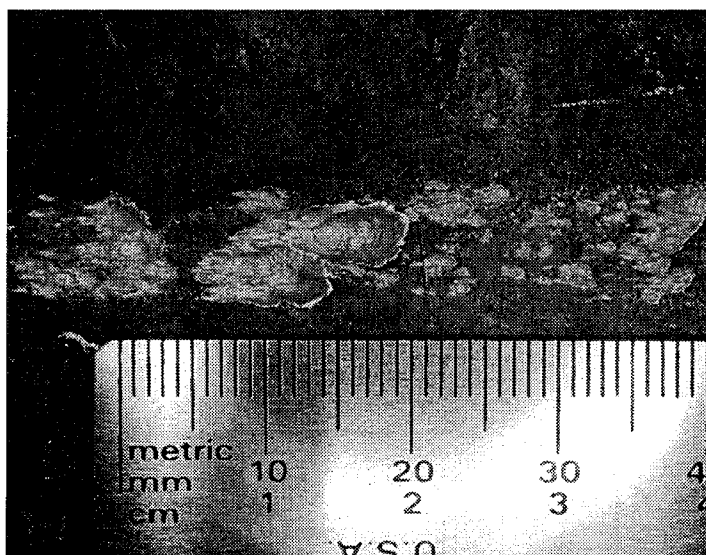
Figure 5.20: "Splash" Gouges Produced at 482 m/s (1580 ft/s) on 3.18 mm (0.125 in) Thick Lead Sheet

More characteristic appearing gouges with a rough interiors were also present on sliding tracks with "splash" gouges. Shown in Figure 5.21 below are gouges produced on the same track but further downstream than those shown in Figure 5.19.
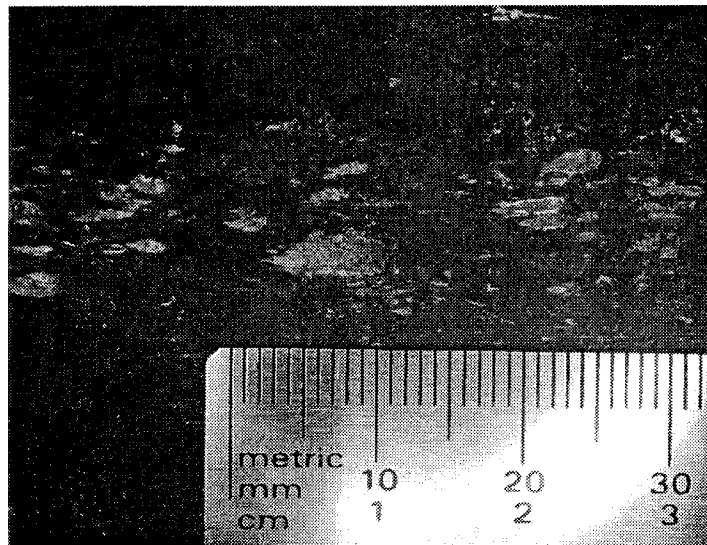
Figure 5.21: Characteristic Gouges Produced at 429 m/s (1406 ft/s) on 3.18 mm (0.125 in) Thick Lead Sheet

Though most gouges produced seemed to develop solely from a point of incidental slider-guider contact, a few of the gouges instead appeared to result directly from scratches or other pre-existing nonuniformities in the surface of the lead sheet guider. Further, a raised manufacturing seam across the entire width of the 3.18 mm (0.125 in) lead sheet used (and thus, because of the way that they were cut, also across every 3.18 mm (0.125 in) guider strip) had the opposite effect. Not only did the seam prevent gouging, but in every case it seemed to cause an extended period where the slider and guider

were not in contact which grew longer as the initial sliding velocity increased. This corresponds with earlier findings in which scratches deliberately placed on a guider target surface resulted in gouges [4,23] but a weld bead deliberately placed across a rail guider surface did not [5,6].

Numerous instances of overlapping gouges were observed. As well, a number of instances were observed where gouges were initiated within the width of a wear track but continued outside of the track. Examples of both of these can be seen in Figure 5.22.
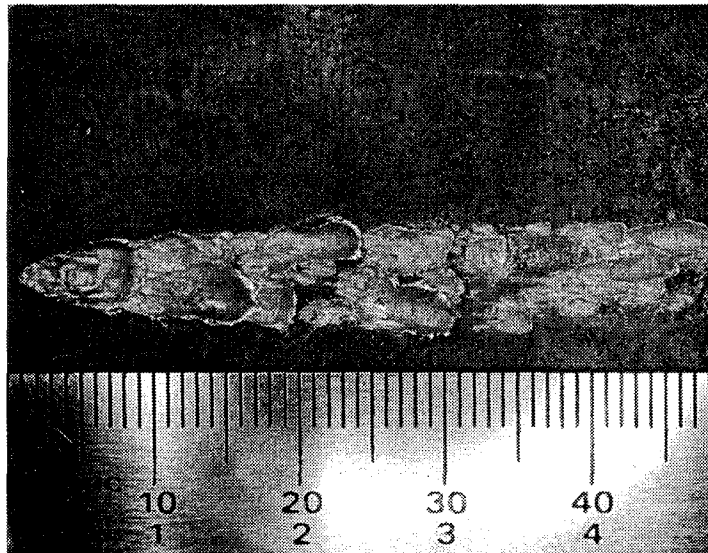
Figure 5.22: Impact Fan, Overlapping Gouges, and Gouges Extending Beyond Width of Wear Track Produced at 429 m/s (1406 ft/s) on 3.18 mm (0.125 in) Thick Lead Sheet

5.2.4 SLIDER DEFORMATION

From the presence of an impact fan and wear track for every shot, it was known that all pellet sliders deformed to some degree upon contact with the lead guider and then continued to move along the surface. What was not initially evident was the extent to which the pellets deformed and whether they actually slid along the guider surface, or instead tumbled and/or broke up. These issues were quickly resolved by examining the pellets which were recovered from sawdust in the bottom of the catch tank after every shot. It was obvious that these recovered pellets had slid. It was also apparent that the degree to which they deformed during the course of impact and sliding depended directly upon the initial sliding velocity. At relatively low initial velocities, the contact surface of the pellet sliders widened and lengthened somewhat, and the overall height with respect to the guider surface was slightly reduced; relatively high initial velocities resulted in the pellets becoming severely deformed and almost flat, as shown in Figures 5.23 and 5.24.
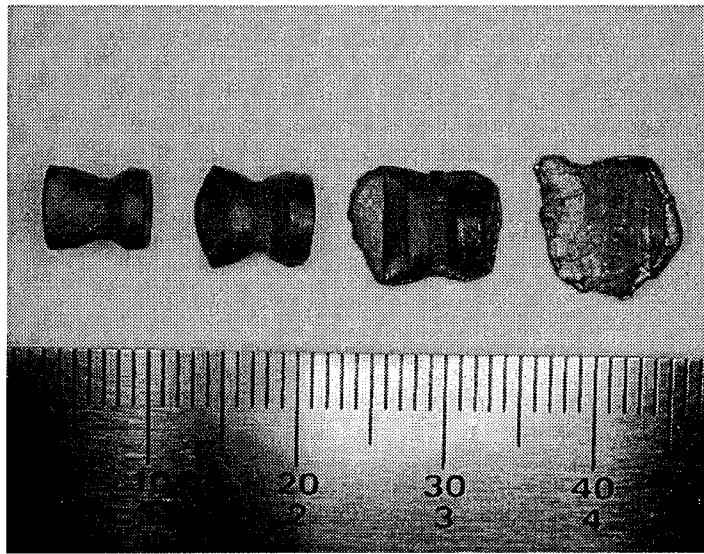
Figure 5.23: View of Pellets Before Sliding and After Sliding at 126 m/s (415 ft/s), 282 m/s (924 ft/s), and 397 m/s (1303 ft/s) (left to right, respectively)
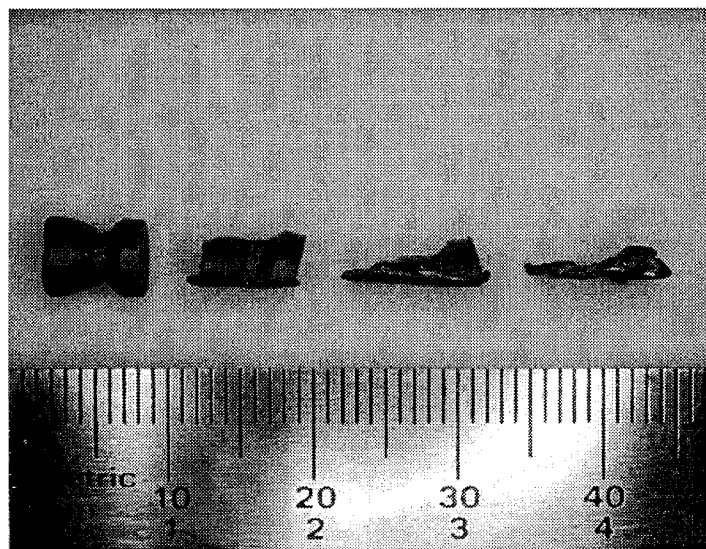
Figure 5.24: Pellet Profile Before Sliding and After Sliding at 126 m/s (415 ft/s), 282 m/s (924 ft/s), and 397 m/s (1303 ft/s) (left to right, respectively)

It is interesting to note that after sliding at any velocity, the sliders were elongated to the rear and their leading edges displayed a protruding, curled lip which grew more pronounced with increasing velocity, as can also be observed in Figure 5.24. While rearward elongation is the logical result of relative motion forcing slider material to the rear, the surprising lip on the leading edge indicates that material was also being pushed forward ahead of the slider.

By weighing the pellets before firing and after sliding, it was known that a loss of slider mass occurred during the experimental process. Slider mass loss was determined to generally increase with an increase in sliding velocity up until the fastest two shots conducted. At 429 m/s (1406 ft/s) and 482 m/s (1580 ft/s), the pellets broke up after impacting and sliding a short distance on the guider, making an accurate determination of mass loss difficult. The relation between slider mass loss and initial sliding velocity is reflected in Figure 5.25 below.
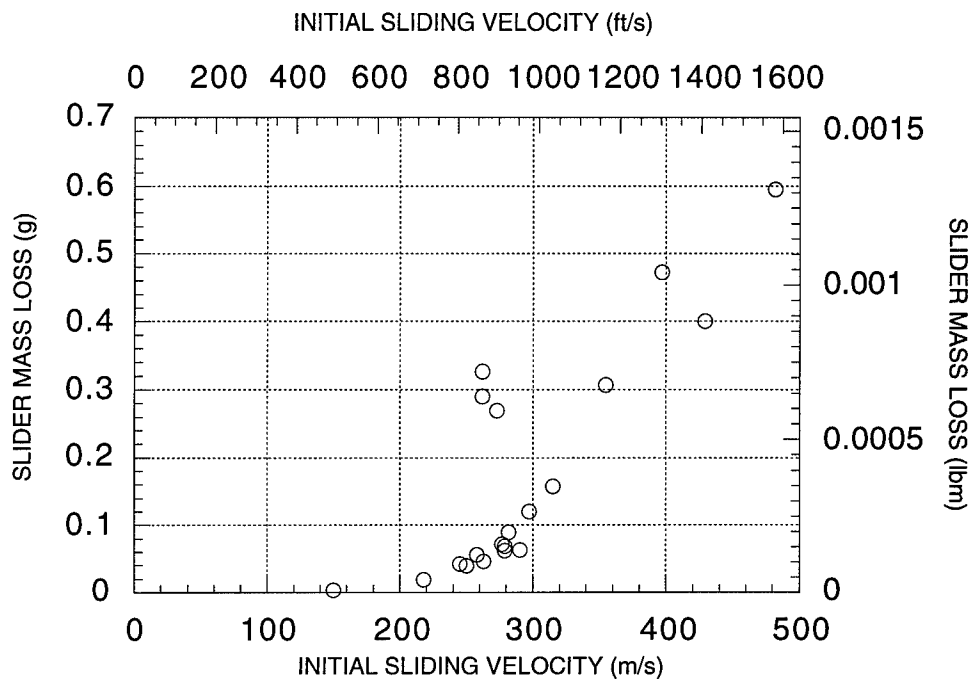
Figure 5.25: Slider Mass Loss versus Initial Sliding Velocity

Though it is conceivable that some projectile mass was lost during acceleration, cleaning between shots indicated minimal accumulation of lead in the barrel. This means that essentially all mass loss occurred during pellet impact and sliding and confirms that the sliding wear tracks were largely due to deposition of slider material onto the guider surface.

Gouging is generally thought to occur simultaneously on the surfaces of the guider and slider. It was hoped that an examination of recovered pellet sliders would provide some confirmation of this. The only way this would really be possible though, was if a gouge on the surface of a slider were so severe that it would not be completely obliterated by additional sliding, or if

no further slider-guider contact occurred after a slider gouge was produced. Unfortunately, gouging never occurred at the very end of the guider surface. and in all cases during deceleration in sawdust (after pellets had left the guider surface), sliding continued for some distance on the inner surface of the steel cylinder. This certainly contributed to slider mass loss as well as resulted in sufficient marring of the sliding surfaces to prevent any meaningful information from being gleaned from them, as shown in Figure 5.26.
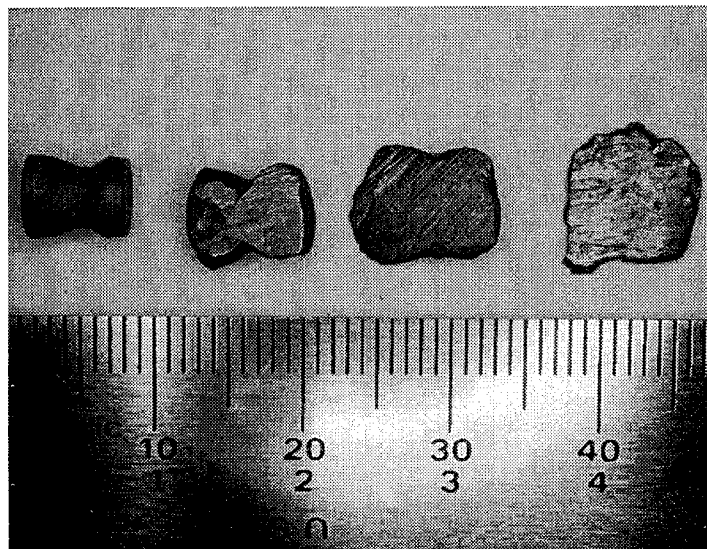
Figure 5.26: Pellet Before Sliding and Pellet Contact Surface After Sliding at 126 m/s (415 ft/s), 282 m/s (924 ft/s), and 397 m/s (1303 ft/s)
(left to right, respectively)

Because of slider surface marring, it can only be speculated that if slider gouging does occur, it must be less severe than that which occurs on the guider. Otherwise, the cumulative effects of all guider gouges from any given wear track, particularly those with large gouges, should have resulted far more slider damage than was observed in any recovered pellet.

5.2.5 EFFECT OF GUIDER THICKNESS AND SURFACE CONDITION

Neither the presence or lack of an oxide layer on the guider surface nor varying the guider thickness seemed to have a significant effect on the appearance of the impact fans, the sliding wear tracks, or upon gouging. Shots 1-6 were conducted with a strip of 3.18 mm (0.125 in) "as is" lead sheet for the guider surface. Shots 7 - 13 were conducted with a strip of 6.35 mm (0.25 in) lead sheet that had been sanded lengthwise with #600 sand paper and water to remove the oxide layer. Shots 14 - 19 were conducted with a strip of 3.18 mm (0.125 in) lead sheet that had been sanded lengthwise with #600 sand paper and water to remove the oxide layer, and then repeatedly dampened and allowed to dry, enabling the oxide layer to reform. Shots 20 - 25 were conducted with a strip of 3.18 mm (0.125 in) "as is" lead sheet. Gouges were produced on both thicknesses of lead sheet used and apparently regardless/in spite of the condition of the oxide layer.

5.3 THE ONSET OF GOUGING

Prior to trying to establish a gouging threshold velocity for lead-on-lead, it was presumed that gouging distinctly either did or did not occur and that there were no intermediate phases of the effect. Gouges were not thought to progress through preliminary stages of development prior to being recognized as gouges. However, in searching the sliding wear tracks for the lowest velocity gouges produced, several instances were observed at low relative velocities in which gouges were present but did not seem fully developed. These "incipient" gouges had characteristics of both the shiny, impact fan gouges described in Section 5.2.1 and more the characteristic gouges described in Section 5.2.3.

5.3.1 INCIPIENT GOUGING

The first instance of "incipient" gouging observed occurred on 6.35 mm (0.25 in) thick lead sheet at 258 m/s (847 ft/s). Here, gouges were produced adjacent to pre-existing scratches in and near the end of the lead guider surface. In these gouges, shown in Figure 5.27 below, while the "tail" regions of the gouges closest to the scratches have the traditional dull, rough appearance, the forward, rounded portions appear shiny yet have the raised edge normally associated with gouging.
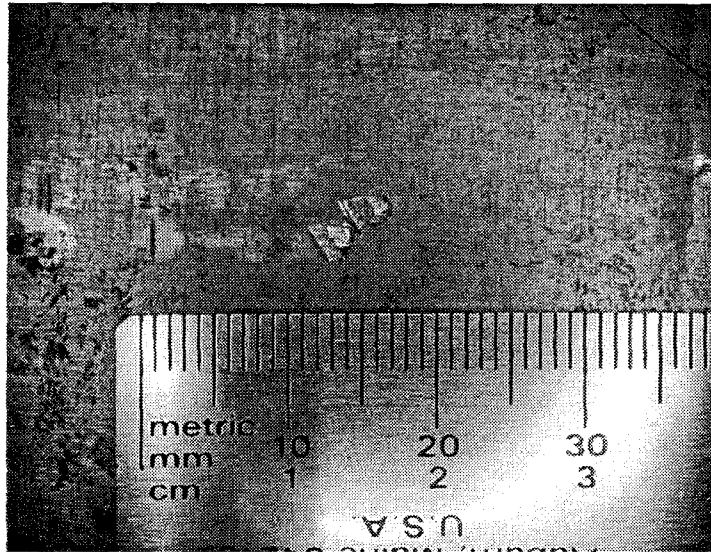
Figure 5.27: Incipient Gouges Produced at 258 m/s (847 ft/s) on 6.35 mm (0.25 in) Thick Lead Sheet

5.3.1 THE GOUGING THRESHOLD VELOCITY

The lowest initial sliding velocity "incipient" gouge observed occurred on 3.18 mm (0.125 in) thick lead sheet at 245 m/s (804 ft/s) and was approximately 3 mm (0.012 in) long and 1 mm (0.004 in) wide. It had an elongated tear-drop shape and the characteristic raised forward edge normally found on gouges. This time though, the forward, rounded portion of the gouge appeared dull and rough while the pointed "tail" portion was shiny. As no other gouges, incipient or otherwise, were produced at a lower initial sliding velocity, 245 m/s (804 ft/s) was determined to be at or near the gouging onset or threshold velocity for lead-on-lead and this particular experimental configuration. This is reasonably close to the predicted gouging onset velocity of 218 m/s (715 ft/s).

95

5.4 A COMPARISON BETWEEN IMPACT FAN GOUGES AND DOWNSTREAM GOUGES

Deformations in the contact fan have previously been ruled from consideration in gouge evaluation [23] and have also been thought important enough to be considered further [15]. Because of this uncertainty surrounding impact fan deformations, during experimentation it was initially thought that gouge-like craters could only be considered bona fide gouges if they occurred on a sliding track downstream from the impact fan. As discussed in Section 5.3.1 though, there appears to be a point of transition in downstream gouges from shiny, striated gouge craters to ones which are dull and rough, similar to the transition observed in impact fan gouges. If this transition in downstream gouges is in fact the point at which characteristic gouges begin to exist, then the same transition observed in impact fans must also indicate the point at which gouges begin to exist. Considered in this light, the dull craters observed in impact fans beginning at 273 m/s (895 ft/s) must be actual gouges. The fact that they begin to appear near the 245 m/s (804 ft/s) gouging threshold velocity established in Section 5.3.1 validates this. A further confirmation of this is that at 482 m/s (1580 ft/s), the single, large impact fan gouge produced appeared identical to other "splash" gouges produced further downstream as can be seen in Figure 5.17.

5.5 LESSONS LEARNED

Many lessons were learned during the course of this experiment. While some served as a confirmation of methods used and choices made, others helped to identify steps which would make a future experiment of a similar nature easier to set up and complete.

5.5.1 REQUIRED SLIDER ACCELERATION CAPABILITY

Before it was known if gouging would be possible at the low relative velocities predicted, it seemed advantageous to have a slider accelerator with the ability to generate initial sliding velocities as close as possible to the known realm of gouging. With a peak muzzle velocity near 500 m/s (1640 ft/s), the helium gun used in this experiment well accomplished that goal (and would have made any small game hunter envious as well!). As it turned out though, the gun was more robust than was necessary to satisfy the demands of the experiment. It would have been far more simple and less time consuming to purchase a commercially available pellet gun rather than have to build one. Premier models for sale boast maximum muzzle velocities of about 335 m/s (1100 ft/s) which is more than enough to explore the gouging threshold of .22 caliber lead pellets on lead sheet.

5.5.2 GUIDER SURFACE PREPARATION

Lead surfaces exposed to air develop a dark, oxide coating. This oxide layer was initially present on all pellets and lead sheet used in the experiment. The dull oxide coating is easily removed from lead sheet with fine sand paper or a scratch pad, revealing a bright, shiny, silver toned surface, but begins to return immediately. Lead also scratches easily. While the pellets used were fairly uniform, both thicknesses of lead sheet used had numerous pre-existing surface scratches and scrapes which were accumulated primarily in transit prior to delivery.

On one hand, both the anomalies and the oxide layer on the lead sheet were beneficial. Deliberately placed irregularities on guider surfaces have been previously reported to prevent gouging (weld beads on a rail [6]) and to cause gouging (scratches and grains of sand [23]). The existing surface defects in lead sheet offered many, fairly randomly located opportunities to validate both of the two theories. Also, as the existing anomalies were oxidized, they were easily distinguished from surface deformations and changes newly acquired during experimentation.

A drawback of the quickly accumulating oxide layer experienced during experimentation was that in air, it was impossible to conduct an iteration of the experiment without the presence of lead oxide at the sliding interface. Further, if the oxide coating was removed, it was impossible to conduct two iterations of the experiment with the same accumulation of oxide. Only using lead sheet in the "as is" condition provided for a consistent presence of the oxide layer during successive iterations of the experiment.

Because of this, the lead guider surfaces used during the course of experimentation had varying accumulations of lead oxide. An inert environment such as helium would have provided a better means of investigating the effect of lead oxide on the gouging of lead sheet.

5.5.3 ATTACHMENT OF GUIDER SURFACES TO THE TARGET CYLINDER

Ideally, no gaps would have existed between the under side of the guider surface and the target cylinder. In reality though, flush attachment of lead strips to the inner surface of the cylindrical catch tank proved difficult to achieve. While the 3.18 mm (0.125 in) thick lead sheet was malleable and easy to shape to the curvature of the cylinder, the 6.35 mm (0.25 in) thick lead sheet was not. Additionally, uniform application of 3M Super Trim Spray Adhesive was difficult to achieve because of the spray's consistency. The desire to remove guider surfaces after they had been used without destroying them, which dictated that a minimum possible amount of the adhesive be used, further compounded this problem. An adhesive that was able to be applied more uniformly and yet still provided for easy removal of the lead sheet would have been a better choice for this experiment. Because the 3.18 mm (0.125 in) thick lead sheet was ultimately easier to work with as well as attach to and remove from the steel target cylinder, it was used for the majority of the iterations of the experiment.

CHAPTER 6

DISCUSSION AND CONCLUSIONS

All of the stated objectives of this thesis and experiment were successfully accomplished. First, laboratory gouging was produced at low velocities relative to those at which it is normally experienced, confirming the validity of the correlation between velocity and slider strength (and accordingly hardness) drawn from reported instances of gouging and extrapolated to a low velocity regime. Specifically, lead was found to gouge at velocities lower than those identified in any previously reported instance of the phenomenon. Next, the gouging onset velocity for lead-on-lead was determined to be at or near 245 m/s (804 ft/s). Lastly, gouges were created inexpensively and in a manner that can be easily reproduced. Even though the experiment was resoundingly successful, proved that gouging can be predicted with reasonable accuracy, and provided much insight into the gouging phenomenon, there are many issues that remain unresolved.

6.1 THE EVOLUTION OF GOUGING

One of the revelations brought about by this experiment is that lead gouges at velocities which are low relative to those at which gouging normally occurs. Almost equally important though is that gouging appears to be a process that evolves from mechanisms already in existence at velocities well below the gouging onset velocity.

As discussed in Section 5.2.2, the contact regions on sliding wear tracks even at velocities as low as 150 m/s (493 ft/s), the lowest initial sliding speed achieved and well below the apparent gouging threshold for lead, often exhibited the characteristic teardrop shape of gouges even though gouging did not occur. As discussed in Sections 5.3 and 5.4, the shiny, striated craters which were observed at velocities as low as 218 m/s (715 ft/s) seemed to develop first into incipient gouges and then ultimately into more traditional gouges as sliding velocity was increased above the gouging threshold velocity. It is apparent then, that the notion of gouging being an effect that distinctly either does or does not occur is incorrect. As can be observed in the impact fans as well as further downstream in the sliding wear tracks, gouging clearly evolves from mechanisms in place well below the threshold velocity which grow progressively more severe as sliding velocity increases. This suggests that given the appropriate material and conditions, gouging may be possible at velocities even lower than those observed with lead.

6.2 LOW VELOCITY GOUGING

Laboratory produced low relative velocity gouging is more than a curiosity. It is very relevant in that it offers a means to investigate unique, high velocity phenomena without the requirement of having highly specialized equipment. Prior to this experiment, research into gouging was limited to those who had large funding, ample time, and access to a railgun, rocket sled, high-velocity gun lab, or hydrocode simulation. This experiment

has proven that gouges can be easily created with limited funds and very ordinary equipment.

There are likely materials other than lead that will also gouge at low relative velocities, as indicated by Figure 6.1 below. This figure reflects the plot originally shown in Figure 3.3 revised to include the gouging onset velocity of lead as determined in this experiment. As with the other curve-fitted plots, this is only an approximation; using the linear relation shown and a yield strength/density value of 2.9 for lead, the onset of gouging would be expected at approximately 230 m/s (755 ft/s) rather than the 245 m/s (804 ft/s) actually experienced in this experiment.
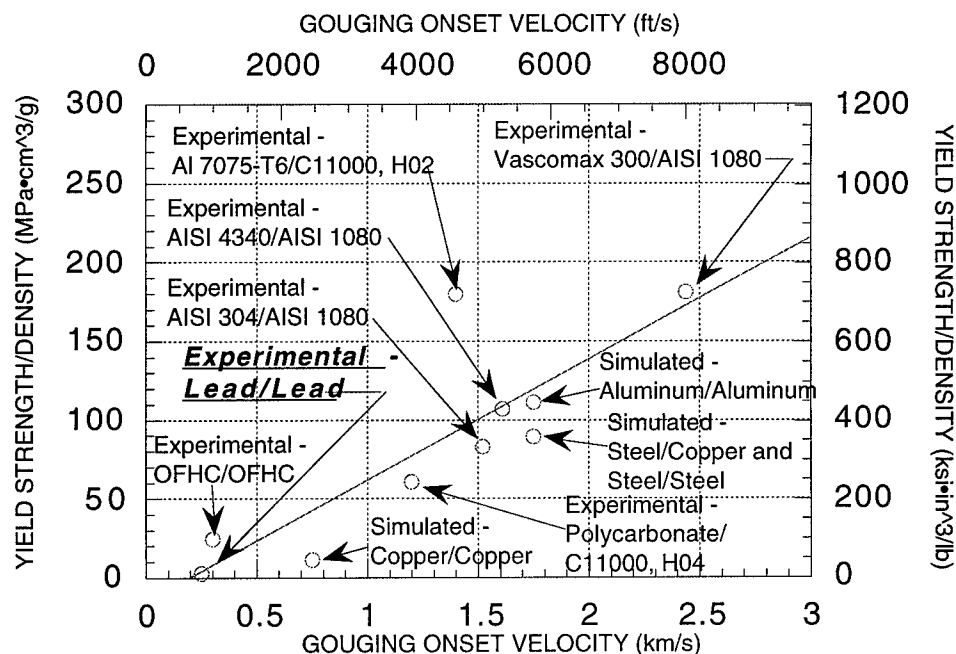
Equation of Linear Curve Fit: $y = -14.80 + 76.92x$ $(R = 0.84)$

Figure 6.1: Revised Experimental and Simulated Slider Yield Strength/ Density versus Gouging Onset Velocity (Slider Material/Guider Material)

102

In accordance with this relation, tin for instance, would be a another likely candidate for low relative velocity gouging. With a yield strength/density value of approximately 3.3 [33], tin would be expected to experience the onset of gouging at a velocity very close to that of lead, at or near 235 m/s (772 ft/s).

It appears unlikely though, that metal gouging is possible at velocities significantly lower than the gouging threshold velocity for lead. To achieve an onset of gouging at a lower velocity than lead and remain in agreement with the above relation, the material would have to have a yield strength/density less than 2.9, and of course be prone to gouging. Even for a (nonexistent) metal with a yield strength/density value equal to 0, the lowest onset velocity this could possibly be is approximately 192 m/s (631 ft/s). Given the error inherent in the linear curve-fit and the fact that this value is not significantly lower that the gouging onset velocity for lead, lead appears to be on the low end of the range of possible metal gouging onset velocities.

However, it may be possible to produce gouge-like effects in some non-metals that have all of the characteristics of gouging. Just as wave-like deformations indicative of high relative velocities have been reproduced on the surfaces of heavy automotive grease and silicon putty with a water jet operating at a much lower velocity [30], it seems reasonable that gouges could be created by means other than tangential sliding contact of metals. The appearance of the "splash" gouges created in this experiment supports the idea that gouge like deformations might be created in the surface of either low melting temperature solids like automotive grease or paraffin wax, or possibly on the surface of a liquid such as water. The appearance and method

of formation of splashes created when a smooth stone is skipped on water are encouraging in this regard and deserve further attention [34,35].

6.3 UNANSWERED QUESTIONS

There remain numerous unanswered questions pertaining to the gouging phenomenon. Among these are the following issues.

6.3.1 THE EFFECT OF SLIDER-GUIDER MATERIAL COMBINATIONS

A question naturally arises out of any relationship quantifying an effect observed in a guider with respect to the material properties of the slider. On what surfaces can a slider of a particular material be expected to produce gouging at the predicted onset velocity? Intuitively, a lead .22 caliber pellet would probably not produce gouges in a steel surface at 245 m/s (804 ft/s) even though it did in a lead surface. In support of this, no gouges were ever observed on the inner surface of the steel target cylinder even though in every iteration of the experiment, after leaving the lead guider surface the lead pellets slid for some distance on steel before coming to a complete stop. Perhaps this is a scaling issue though, and a much larger and heavier lead slider would gouge steel at 245 m/s (804 ft/s). Unfortunately, scaling of impact related events is in itself a complex issue. Even the most promising empirical scaling theories, one of which eliminates the importance of the projectile in defining the impact process, contain constants which are unknown or difficult to estimate [36]. This leaves physical models, such as

104

hydrocode simulations, the most certain way to determine if the linear relation established during the course of this research holds true for systems of different sizes [36,37].

This issue merely highlights the fact that the relation in Figure 3.3 does not relate the properties of a slider with those of the guider surface. After initially determining that slider yield strength and hardness were the material properties that seemed to correlate with gouging onset velocity, it was attempted to address this problem by drawing a similar, meaningful relationship contrasting slider properties to guider properties. An example of this is shown in Figure 6.2.

Figure 6.2: Slider/Guider Yield Strength Ratio versus Gouging Onset Velocity (Slider Material/Guider Material)
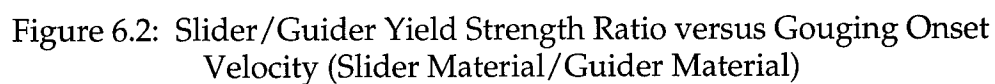
A number of observations can be drawn from this plot. It was already known that in many of the instances of gouging reported, the slider and guider were identical or similar materials. It is no surprise then, that many of the data points have a slider-guider yield strength ratio at or near 1. For all gouging slider-guider combinations, slider yield strength is always equal to or greater than the guider yield strength. This could be significant or merely may reflect a natural tendency from a design standpoint for dynamic parts be stronger than those that are static.

Ultimately, no relationship could be found that related the gouging onset velocity to slider properties and guider properties. This leaves the issue of the interactive effect of slider and guider materials unresolved.

6.3.2 THE EFFECT OF HIGH CURRENT DENSITIES

Neither in this nor any previous study of the gouging phenomenon has the issue of the effect of high current densities on gouging been addressed. Instances of railgun gouging have been "lumped" together with other instances of gouging while a fundamental difference in the systems in which the gouging occurred has not been addressed. Specifically, in railguns, current in the megamp range is flowing through the armature-rail (slider-guider) interface while gouging occurs [16]. It is well known that the Joule or ohmic heating generated by these current densities contributes significantly to the temperature rise at the armature-rail interface [17-19]. What is not known is the effect that this has upon gouging. Though illogical, it is possible

106

that high current density has little or no impact upon the formation and propagation of gouges. If this is in fact true, it seems reasonable to expect that the linear relation between gouging onset velocity and the quotient of slider yield strength and density established in Section 3.1.5 would remain essentially unchanged if railgun data points were neglected. Figure 3.3 was modified accordingly with the result appearing in Figure 6.3.

GOUGING ONSET VELOCITY (ft/s)
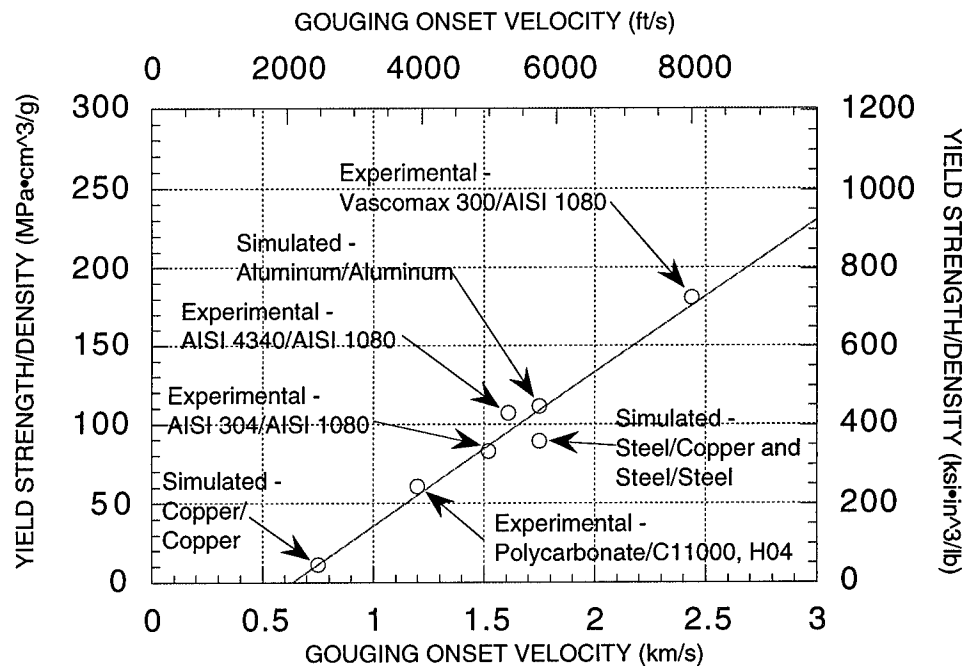
Equation of Linear Curve Fit: y = -61.46 + 97.40x (R = 0.98)

Figure 6.3: Experimental and Simulated Slider Yield Strength/Density versus
Gouging Onset Velocity With Railgun Data Omitted
(Slider Material/Guider Material)

While the relation in this plot differs from the original, with little deviation of data points from the linear curve fit and a correlation coefficient of R = 0.98, it actually provides a more convincing argument than the original relation of a linear relationship between the quotient of yield strength and density and the gouging onset velocity. Unfortunately, this new relation also predicts the gouging onset velocity of a lead slider to be at or near 661 m/s (2167 ft/s), well above both the originally predicted value of 218 m/s (715 ft/s) and the experimentally determined value of 245 m/s (804 ft/s).

A more accurate prediction of gouging onset velocity seems to occur when all instances of gouging are "lumped" and considered together rather than by omitting railgun data points. However, this defies logic by indicating that high current densities have little if any effect on the gouging onset velocity of a conducting slider material. From these data points and the results of this experiment alone then, the effect of high current densities upon gouging remains uncertain.

6.3.3 GOUGING AND THE HYPERVELOCITY REGIME

Gouging has previously been thought of as predominantly a hypervelocity phenomenon. However, in this experiment, it has been shown that gouges can be consistently reproduced at velocities well below 1 km/s (3281 ft/s) which is generally thought of as the lower limit of the hypervelocity regime. More exacting definitions of hypervelocity can be found in discussions of impact dynamics. Hypervelocity impact has been described as the regime in which hydrodynamic pressure dominates the

108

behavior of colliding solids. This occurs because at striking velocities significantly greater than the local sound speed of the target material, shock waves propagate through the bodies which, for all practical purposes behave as fluids [38]. In the case of lead, both the elastic longitudinal and shear wave speeds, approximately 2.0 km/s (6562 ft/s) and 890 m/s (2920 ft/s), respectively [39,40], are well above the velocity at which gouging begins to occur. This would seem to indicate that gouging, in lead at least, is not a hypervelocity phenomenon.

Another method of characterizing impacts is a dimensionless value called the damage number "D," where [46]:

$$D = \frac{\rho V^2}{Y} \qquad (6.1)$$

and ρ = target material density

V = impact velocity

Y = target material yield stress

The hypervelocity regime is characterized as having values of D >1000 [46]. Even if the initial slider-guider contact in this experiment had been normal (angle of incidence of 90 degrees), at the gouging onset velocity of lead 245 m/s (804 ft/s), the largest damage number possible would be:

$$D = \frac{(11.35 \text{g} / \text{cm}^3)(245 \text{m} / \text{s})^2}{11000 \text{kPa}} \qquad (6.2)$$

or

$$D \approx 62$$

109

This is not near the hypervelocity regime. Rather, it corresponds to the "high velocity" or "ordnance" realm where $1 < D < 100$ [46]. Accordingly, this definition would also lead one to question whether the gouging of lead can accurately be described as a hypervelocity phenomenon.

On the other hand, perhaps gouging is strictly a hypervelocity phenomenon and the real issue is in the definition of hypervelocity. Another description of hypervelocity characterizes the "hypervelocity sliding threshold velocity" as the velocity at which the stress induced by slider-guider asperity impact is equal to the ultimate stress of the material involved [1]. In this discussion, it is stated that the onset of gouging of copper railgun rails at the ANU is consistent with this definition in that by 300 m/s (984 ft/s), all but the most oblique impacts (of less than 5 degrees) will produce stresses at or above the ultimate strength of copper. Using the same definition and reasoning, the onset of gouging in lead would be expected to occur at sliding velocities below 40 m/s (131 ft/s). While well below the gouging onset velocity observed in this experiment, this figure indicates that 245 m/s (804 ft/s) is well within the hypervelocity regime for lead.

Whether or not gouging can be classified as a hypervelocity phenomenon, then, is uncertain. The only thing clear from these discussions, previous work done on gouging, and this experiment is that magnitude of normal force generated during slider-guider contact is critical in defining hypervelocity and in the onset of gouging.

6.3.4 THE RELATIONSHIP BETWEEN SLIDER NORMAL FORCE AND GOUGING ONSET VELOCITY

In previous studies of the gouging phenomenon, it is generally agreed that in addition to sliding velocity, a nominal amount of normal force at a slider-guider interface, relative to the properties of the materials involved, is required for gouging to occur. This normal force has been attributed to slider-guider surface asperity impact [1], gouge initiating particles [8,9], and normal slider velocity components [2]. The fact that appropriate curvature was required in the target/guider surfaces in this and previous gouge producing experiments [4,23] further confirms the requirement of a "sufficient" amount of normal force for gouges to occur. In reality then, the gouging onset velocity is a function of normal force as well as slider material properties. For this reason, it seems appropriate as well as more accurate to describe gouging and its onset velocity for a given slider material in terms of the normal force required for gouging. At present there is no data which either quantifies "sufficient" normal force or specifically relates slider normal force to gouging or the gouging onset velocity. It is conceivable though, that a relationship between slider normal force and gouging onset velocity does exist for every slider material prone to gouging and that this relationship defines the "gouging window" for that material.

If it is presumed that the normal forces which cause gouging are functions of slider characteristics and are transmitted to the guider surface through asperity impact, it follows that the magnitude of transmitted force can be altered by varying the slider mass, the slider normal acceleration, the

111

slider tangential velocity, or any combination of the three. It also follows that there exist many combinations of the three would result in the same magnitude of transmitted normal force. Accordingly, it is speculated that within a slider's "gouging window," different combinations of slider velocity and normal force could be expected to produce gouging with gradually less slider normal force being required as sliding velocity is increased. Similarly, the apparent gouging onset velocity for a slider of a particular material could be raised or lowered by raising or lowering the resultant slider normal force. Stated differently, gouging by lead sliders may be possible at velocities lower than 245 m/s (804 ft/s) by using either a slider with more mass than a .22 caliber "wadcutter" pellet or a target surface with a radius of curvature less than the 43.18 cm (17.0 in) used in this experiment so that greater slider normal acceleration is generated. Also, with increasing sliding velocity, sliders with progressively less mass and/or normal acceleration should still produce gouging within the "window," the upper limit of which is determined by melting of the slider-guider contact surfaces and was not experimentally observed. Beyond a gouge window's upper limit, no amount of applied normal force would produce any further gouging. This speculated relationship between slider velocity and slider normal force is reflected in Figure 6.4.
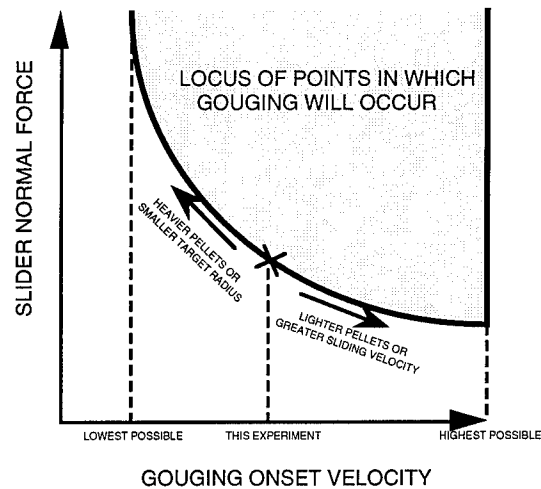
Figure 6.4: A Speculative Gouging "Window"

Similarly, it is speculated that there exists a relationship between the gouging onset velocity, slider normal force, and slider yield strength. This relationship, which combines the linear correlation between slider yield strength/density and gouging onset velocity established in this experiment and the relation hypothesized above, would relate the nominal gouging onset velocity for a slider of a given yield strength/density to the normal force required for gouging to occur.

113

6.4.5 OTHER ISSUES

There are many other questions which prevent the gouging phenomenon from being fully understood. Among these are the following:

1. Do gouges actually develop on sliders simultaneously with those that form on the guider? If so:

    1.1. How does the size of slider gouges compare to the gouges generated on a guider ?

    1.2. How does the loss of slider volume compare or scale to the loss of guider volume?

2. What happens to the volume of material removed from a gouge?

3. Railgun armatures do not have a "free surface" as do rocket sled shoes, so pressure relief in the sliders is different. How does this affect simulation models?

4. Can gouges or gouge-like effects be created on the surface of non-metals?

6.5 RECOMMENDATIONS FOR FURTHER RESEARCH

There are numerous avenues of research that would help to clarify the unresolved issues identified in Sections 6.3 and 6.4. The following are a few recommendations.

1. Additional data points which reflect instances of gouging at low relative velocities would further validate the linear correlation between slider yield strength/density and gouging onset velocity. These could be experimentally created with the method used during the course of this research. Tin, with a yield strength/density value of approximately 3.3 [33]would be a logical for candidate for low velocity gouging. As discussed in Section 6.2, tin slider would be expected to experience the onset of gouging at a sliding velocity at or near 235 m/s (772 ft/s).

2. With careful control of an experiment similar to the one conducted during the course of this research, the existence of the speculated relationship between gouging onset velocity and slider normal force discussed in Section 6.3.4 could easily be confirmed or denied. This could be done with some difficulty by varying slider mass while holding initial sliding velocity constant, or more simply by using a variable-curvature target (or a series of targets with varying curvature) and holding initial sliding velocity and slider mass constant.

3. Even though temperatures at sliding interfaces are considerably higher than room temperature, during this study only room temperature data was considered in establishing the linear relationship between slider yield strength and gouging onset velocity. No consideration was given to known or predicted slider-guider interface temperatures in documented instances of gouging. At a minimum, estimated temperatures could and should be used to determine if the linear correlation between gouging onset velocity and slider yield strength/density holds true at higher temperatures and to determine if any other gouging onset velocity - material property relations exist. Elevated temperature data should also serve as the basis for further study of the interactive effect of slider and guider materials and be used to determine if there exists a relationship between slider properties, gouging onset velocity, and guider properties.

4. Related to the use of elevated temperature data is the effect of high current densities upon the onset and propagation of gouging. No model of gouging is complete unless it encompasses and analyzes the effect of high current density. For this reason, a computer simulation which could "produce" gouges with and without current effects would be a more accurate model than those which have previously been used to replicate gouging. The development of such a model would also be a useful tool in railgun design, as would a model that considered slider-guider contact at multiple sliding surfaces (armature contact on two rails simultaneously).

116

6.5 CONCLUSION

During this study, the onset of surface gouging by metals in sliding contact which usually occurs in rocket sleds, two-stage gas guns, and electromagnetic railguns and at sliding velocities in excess of 1,000 m/s (3,281 ft/s) has been shown to vary linearly with the quotient of yield strength and density of the slider material. This linear relationship was used to predict with reasonable accuracy the onset velocity of gouging for a slider of a chosen material on a material never before reported to have gouged, and to show that gouging is possible at sliding velocities less than those at which it is normally observed. Specifically, gouging was produced in a laboratory experiment with a lead slider and lead guider at velocities as low as 245 m/s (804 ft/s), well below the onset velocity in any previously reported instance of the phenomenon.

These results are significant for a number of reasons. First, if the onset of gouging can be accurately predicted, it can also be avoided. As gouging is an undesirable side-effect in systems normally involving high velocity sliding, the ability to avoid gouges is a beneficial skill and one which is analogous to preventing gouges. Second, because it has been shown that gouging can occur or be produced at low relative sliding velocities, research into the causes of and mechanisms involved in gouging is no longer restricted to those with access to rocket sleds, railguns, or super computers. All of these assets are also usually too expensive, large, complex, and in demand to allow them to be dedicated to the production and/or study of gouges. Essentially, it has been shown that anyone with a standard, commercially available pellet

117

gun, lead pellets, and a sheet of lead can produce gouges almost at will. With slightly more equipment, an in depth analysis of gouging becomes possible. Third, the fact that gouging has been demonstrated at low sliding velocities relative to those at which it normally occurs suggests that gouging or gouge like effects may be possible at even lower velocities and/or in different mediums.

Unfortunately, there still remain many unanswered questions pertaining to gouges and their formation. Until these are resolved, gouging will remain a phenomenon.

APPENDIX A:

PROPERTIES OF MATERIALS INVOLVED IN DOCUMENTED INSTANCES OF GOUGING

MATERIAL	"COPPER" (PURE?) (SEE #1)	COPPER, OFHC(?)	COPPER, C11000 H02	COPPER, C11000 H04	"STEEL" (AISI 4140? (4150)) (SEE #1 & 2)	STEEL, AISI 1080 (1095)	STEEL, AI3I 4340 (4330)	STEEL, AISI 304 (STAINLESS)	STEEL, MARAGING (VASCOMAX 300)	"ALUMINUM" (PURE)	ALUMINUM, 7075-T6	PLASTIC, POLYCARBONATE	LEAD
REFERENCE WHERE GOUGING INVOLVING THIS MATERIAL IS CITED	[10,11]	[1]	[29]	[12]	[10,11]	[5,6,15]	[15]	[5,6]	[15]	[10,11]	[29]	[12]	N/A
HUGONIOT ELASTIC LIMIT, HEL (Gpa)	0.6 [40]	0.6 [40]	0.6 [40]	0.6 [40]	3.7 [40]	2.1 [40]	-	0.2 [40]	2.8 [40]	-	-	-	0 [40]
BULK WAVE SPEED, Cb (km/s)	3.94 [10,11]	3.93 [39]	3.93 [39]	3.93 [39]	4.59 (#3)	-	-	4.507 [39]	4.36 (#3)	5.42 [10,11]	5.13 [39]	1.929 [39]	2.002 [39]
LONGITUDINAL WAVE SPEED (IN SLIM BAR), Co (km/s)	3.91 [39]	3.91 [39]	3.91 [39]	3.91 [39]	-	-	-	4.58 [39]	-	5.1 [21]	5.2 [39]	-	2.03 [39]
LONGITUDINAL WAVE SPEED (=CO IN INFINITE BODY), Cl (km/s)	4.76 [40]	4.76 [40]	4.76 [40]	4.76 [40]	5.89 [40]	-	-	5.77 [40]	5.54 [39]	6.1 [21]	6.394 [21]	2.18 [39]	2.25 [39]
SHEAR WAVE SPEED, Cs (km/s)	2.33 [40]	2.33 [40]	2.33 [40]	2.33 [40]	3.2 [40]	-	-	3.12 [40]	2.96 39]	-	3.109 [21]	0.88 [39]	0.89 [39]
POISSON'S RATIO	0.343 [21]	0.343 [21]	0.33 [42]	0.33 [42]	0.288 [43]	0.288 [43]	0.288 [43]	0.305 [43]	-	0.345 [21]	0.33 [42]	-	0.425 [43]
k	0.933 (#4)	0.933 (#4)	0.931 (#4)	0.931 (#4)	0.924 (#4)	-	-	0.927 (#4)	-	0.933 (#4)	0.931 (#4)	-	0.945 (#4)
RALEIGH WAVE SPEED, Cr (km/s)	2.17 (#4)	2.17 (#4)	2.17 (#4)	2.17 (#4)	2.96 (#4)	-	-	2.89 (#4)	-	-	2.9 (#4)	-	0.84 (#4)
DENSITY (Mg/m^3)or(g/cm^3)	8.94 [10,11]	8.924 [39]	8.89 [42]	8.89 [42]	7.785 [40]	7.84 [46]	7.85 [44]	7.89 [39]	8.0 [41]	2.7 [10,11]	2.804 [39]	1.193 [39]	11.349 [33]
SURFACE ENERGY (erg/cm^2)/	1100 [28]	1100 [28]	1100 [28]	1100 [28]	1500 [28]	1500 [28]	1500 [28]	1500 [28]	-	900 [28]	900 [28]	-	450 [28]
YIELD STRENGTH @ 24 C/75 F (MPa)													
HIGH	-	365 [42]	250 [42]	310 [42]	-	869 [41]	972 [41]	655 [41]	2135 [41]	-	-	-	55 [33]
LOW	-	69 [42]	250 [42]	275 [42]	-	370 [41]	710 [41]	655 [41]	758 [41]	-	-	-	11 [33]
AVGERAGE	100 [10,11]	217	250	292.5	700 [10,11]	619.5	841	655	1446.5	300 [10,11]	503 [42]	72.5 [44]	33
ULTIMATE (TENSILE) STRESS @ 24 C/75 F (MPa)													
HIGH	445 [42]	445 [42]	-	345 [42]	1020 [41]	1270 [41]	1448 [41]	-	2169 [41]	-	-	-	62 [33]
LOW	221 [42]	221 [42]	-	310 [42]	814 [41]	615 [41]	1110 [41]	-	1034 [41]	-	-	-	14 [33]
AVGERAGE	333	333	290 [42]	327.5	917	942.5	1279	960 [41]	1446.5	128 [42]	572 [42]	100 [44]	38
HARDNESS (HB)													
HIGH	62 [42]	62 [42]	-	50 [42]	302 [41]	352 [41]	[41]	-	[41]	-	-	-	17 [33]
LOW	10 [42]	10 [42]	-	45 [42]	241 [41]	174 [41]	321 [41]	-	301 [41]	-	-	-	4.7 [33]
AVERAGE	36	36	40 [42]	47.5	271.5	263	354.5	277 [41]	430.5	35 [42]	150 [42]	110 [44]	10.85 [33]
ELASTIC MODULUS, E (GPa)	117	117	125	125	200	205	200	193	190	69.1	71	5.8 [44]	20 [33]
APPROX. MELTING TEMP or RANGE (C)	1083 [42]	1082.3 [42]	1083 [42]	1083 [42]	1460 [41]	1335 [43]	1400 [44]	1427 [43]	-	660.3 [42]	555 [42]	220 [44]	327 [43]
AVG COEFF THERM EXP 20 - 100 C (um/m•K@C)	17 [42]	15.9 [42]	17 [42]	17 [42]	12.2 [42]	11 [41]	11.5 [41]	17 [41]	10.1 [41]	23.6 [42]	23.6 [42]	44 [44]	16.15 [33]
THERM COND @ 20 C (W/M•K@C)	392.8 [42]	392.8 [42]	388 [42]	388 [42]	49 [42]	48 [41]	49 [41]	26 [41]	25.3 [41]	222.12 [42]	130 [42]	1.38 [44]	17.8 [33]
SPECIFIC HEAT J/kg•K@20 C	400 [42]	385 [42]	385 [42]	385 [42]	470 [42]	490 [41]	-	502 [41]	-	900 [42]	962 [42]	1255 [44]	130 [28]
YIELD STRENGTH/DENSITY	11.19	24.32	28.12	32.90	89.17	79.02	107.13	83.02	180.81	111.11	179.39	60.77	2.91

NOTES:
#1: Material type was not specified so it was approximated by this type by matching properties that were given
#2: Properties unavailable for specified (or approximated) material were approximated by material in parentheses
#3: Value shown was calculated as shown in [39]
#4: Value shown was calculated as shown in [21]

REFERENCES

[1] J. P. Barber and D. P. Bauer, "Contact Phenomena at Hypervelocities," *Wear* **78** (1982), pp. 163-169.

[2] R. D. M. Tachau, "An Investigation of Gouge Initiation in High-Velocity Sliding Contact," Ph.D. Dissertation, Department of Aerospace Engineering and Engineering Mechanics, University of Texas at Austin, August 1991.

[3] R. D. M. Tachau, C. H. Yew, and T. G. Trucano, "Gouge Initiation in High-Velocity Rocket Sled Testing," To be published in *International Journal of Impact Engineering*, Vol. 17, Elsevier Science Publishers, 1995, pp. 825 - 836.

[4] K. F. Graff and B. B. Dettloff, "The Gouging Phenomenon Between Metal Surfaces at Very High Sliding Speeds," *Wear* **14** (1969), pp. 87-97.

[5] F. P. Gerstle, P. S. Follansbee, G. W. Pearsall, and M. L. Shepard, "Thermoplastic Shear and Fracture of Steel During High-Velocity Sliding," *Wear* **24** (1973), pp. 97-106.

[6] F. P. Gerstle, "Deformation of Steel During High Velocity Unlubricated Sliding Contact," Ph.D. Dissertation, Department of Mechanical Engineering , Duke University, January 1972.

[7] F. P. Gerstle and G. W. Pearsall, "The Stress Response of an Elastic Surface to a High-Velocity, Unlubricated Punch,' *Transactions of the ASME*, December 1974, pp. 1036 - 1040.

[8] L. M. Barker, T. G. Trucano, and J. W. Munford, "Surface Gouging by Hypervelocity Sliding Contact Between Metallic Material," Sandia Report SAND 87-1328 UC-34, Sandia National Laboratories, September 1987.

[9] L. M. Barker, T. G. Trucano, and J. W. Munford, "Surface Gouging by Hypervelocity Sliding Contact," in *Shock Waves in Condensed Matter 1987* (edited by S. C. Schmidt and N. C. Holmes), Elsevier Science Publishers, 1988, pp. 753 - 756.

[10 L. M. Barker, T. G. Trucano, and A. R. Susoeff, "Gun-Barrel Gouging by Sliding Metal Contact at Very High Velocities," Sandia Report SAND 88-2786C, Sandia National Laboratories, 1988.

[11] L. M. Barker, T. G. Trucano, and A. R. Susoeff, "Railgun Rail Gouging by Hypervelocity Sliding Contact," *IEEE Transactions on Magnetics*, Vol. 25, No. 1, January 1989, pp. 83 - 87.

[12] A. R. Susoeff and R. S. Hawke, "Mechanical Bore Damage in Round Bore Composite Structure Railguns," Lawrence Livermore National Laboratory, UCID-21520, February 10, 1988.

[13] R. D. M. Tachau, "High-Velocity Reverse Ballistic Rocket Sled Testing at Sandia National Laboratories," *The Shock and Vibration Bulletin*, NO. 57, Part 2, pp. 99 - 104.

[14] G. L. Ferguson, "Dynamic Analysis of a Sled Traveling Along a Rough Rail," Ph.D. Dissertation, New Mexico State University, May 1985.

[15] D. J. Krupovage, "Rail Gouging on the Holloman High Speed Test Track," 6585th Test Group, Test Track Division, Holloman AFB, NM, September 1984.

[16] W. F. Weldon, "Development of Hypervelocity Electromagnetic Launchers," *International Journal of Impact Engineering*, Vol. 5, 1987, pp. 671-679.

[17] R. A. Marshall, "The Mechanism of Current Transfer in High Current Sliding Contacts," *Wear* **37** (1976), pp. 233 - 240.

[18] E. Rabinowicz, "The Temperature Rise at Sliding Electrical Contacts," *Wear* **78** (1982), pp. 29 - 37.

[19] C. Persad and D. R. Peterson, "High Energy Modification of Surface Layers of Conductors," *IEEE Transactions on Magnetics*, Vol. MAG-22, No. 6, November 1986, pp. 1658 - 1661.

[20] A. C. Mueller and E. M. Fernando, "The Dynamics of Projectiles Launched By A Two-Stage Light-Gas Gun," DTIC Report AD-A274 380, Arnold Engineering Development Center, Arnold AFB, Tennessee, November 1991.

[21] M. A. Meyer, <u>Dynamic Behavior of Material</u>, John Wiley & Sons, Inc., New York, 1994, pp. 38, 40 - 42, 319.

[22] L. M. Barker, M. Shahinpoor, and L. C. Chhabildas, "Experimental and Diagnostic Techniques," in <u>High-Pressure Shock Compression of Solids</u>, (edited by J. R. Asay and M. Shahinpoor), Springer-Verlag, New York, 1992, p. 48.

[23] K. F. Graff, B. B. Dettloff, and H. A. Bobulski, "Study of High Velocity Rail Damage," Department of Engineering Mechanics, Ohio State University Research Foundation, Air Force Missile Development Center, Holloman Air Force Base, New Mexico, November 1968.

[24] K. F. Graff and B. B. Dettloff, "Study of High Velocity Rail Damage," Department of Engineering Mechanics, Ohio State University Research Foundation, Air Force Special Weapons Center, Kirtland Air Force Base, New Mexico, August 1970.

[25] F. P. Bowden and E. H. Frietag, "The friction of solids at very high speeds I. Metal on metal; II. Metal on diamond," *Proceedings of the Royal Society of London*, Ser. A, Vol. 248, 1958, pp. 350 - 367.

[26] F. P. Bowden, F. R. S., and P. A. Persson, "Deformation, heating and melting of solids in high-speed friction," *Proceedings of the Royal Society of London*, Ser. A, Vol. 261, 1961, pp. 433 - 458.

[27] G. R. Abrahamson and N. J. Goodier, "The Hump Deformation Preceding a Moving Load on a Layer of Soft Material," *Journal of Applied Mechanics*, December 1961, pp. 608 - 610.

[28] E. Rabinowicz, <u>Friction and Wear of Materials</u>, John Wiley & Sons, Inc., New York, 1965, pp. 32-36, 235.

[29] R. A. Marshall, "Multi-Point Packed Wire, and Monolithic Armatures," *IEEE Transactions on Magnetics*, Vol. 31, No. 1, January 1995, pp. 209 - 213.

[30] G. R. Abrahamson, "Permanent Periodic Surface Deformations Due to a Traveling Jet," *Journal of Applied Mechanics*, December 1961, pp. 519 - 528.

[31] R. V. Giles, J. B. Evett, and C. Liu, <u>Schaums Outline of Theory and Problems of Fluid Mechanics and Hydraulics 3/ed</u>, McGraw-Hill, Inc., New York, 1994, pp. 234 - 236.

[32] F. M. White, <u>Fluid Mechanics</u>, McGraw-Hill Book Company, New York, 1979, pp. 513 - 586, 679.

[33] R. Stedfeld (editor), "Comparison of Materials," in *Materials Engineering*, December 1990, pp. C1 - C19.

[34] C. L. Strong, "The Amateur Scientist," *Scientific American*, August 1968, pp. 112 - 118.

[35] H. R. Crane, "How Things Work - What Can a Dimple Do for a Skipping Stone," *The Physics Teacher*, May 1988, pp. 300 - 301.

[36] E. V. C. Ryan, "Catastrophic collisions: Laboratory impact experiments, hydrocode simulations, and the scaling problem," Ph.D. Dissertation, Department of Geosciences, University of Arizona, 1992.

[37] K. A. Holsapple, "The Scaling of Impact Phenomenon," *International Journal of Impact Engineering*, Vol. 5, 1987, pp. 343 - 355.

[38] J. A. Zukas, "Stress Waves and Fracture'" in <u>Material at High Strain Rates</u> (edited by T. Z. Blazynski), Elsevier Applied Science, London and New York, 1987, p. 220.

[39] S. P. Marsh (editor), <u>LASL Shock Hugoniot Data</u>, University of California Press, Ltd., London, England, 1980, pp. 4, 57, 100, 184, 212.

[40] C. E. Morris (editor), <u>Los Alamos Shock Wave Profile Data,</u> University of California Press, Ltd., London, England, 1982, pp. 37, 94, 123, 126, 477 - 480.

[41] P. D. Harvey (editor), <u>Engineering Properties of Steel</u>, American Society for Metals, Metals Park, Ohio, 1982, pp. 41 - 43, 113 - 116, 130 - 136, 273 - 277, 477, 488.

[42] <u>Metals Handbook Tenth Edition Volume 2 Properties and Selection: Metals and Alloys</u>, American Society for Metals, Cleveland, 1990, pp. 45 - 117, 217 - 275.

[43] T. Baumeister, <u>Marks's Standard Handbook for Mechanical Engineers,</u> <u>Eighth Edition</u>, McGraw-Hill Book Company, New York, 1978, p. 6-11.

[44] D. G. Ullman, <u>The Mechanical Design Process</u>, McGraw-Hill Inc., New York, 1992, pp. 300 - 316.

[45] J. E. Field and I. M. Hutchings, "Surface Response to Impact'" in <u>Material</u> <u>at High Strain Rates</u> (edited by T. Z. Blazynski), Elsevier Applied Science, London and New York, 1987, p. 243 - 293.

[46] L. H. Van Vlack, <u>Elements of Materials Science and Engineering, Fourth</u> <u>Edition</u>, Addison-Wesley Publishing Company, 1980, pp. 522, 523.

[47] R. A. Marshall, "Moving Contacts in Macro-Particle Accelerators," in *HIGH POWER HIGH ENERGY PULSE PRODUCTION AND APPLICATION - THE PROCEEDINGS OF AN AUSTRALIAN - US SEMINAR ON ENERGY STORAGE, COMPRESSION AND SWITCHING, SESCAS '77* (edited by E. K. Inall), ANU Press, Canberra, 1978.

VITA

Kenneth Robert Tarcza ████████████████████████████
████████ the son of Robert and Elsie Tarcza and the grandson of
Hungarian immigrants. After graduating from George C. Marshall High
School in 1981, he entered the United States Military Academy. In May
1985, he graduated from West Point with a Bachelor of Science in
Mechanical Engineering and was commissioned as a Second Lieutenant of
armor. After an assignment with the 3rd Infantry Division in Germany
where he met his future wife, he returned to the United States and
married the former Margaret Elizabeth████ on July 1, 1989. Subsequent
assignments took him and his wife to Fort Knox, Kentucky for one year,
and then to the 1st Cavalry Division at Fort Hood, Texas, where he spent
three and one-half years, including a six month tour in Southwest Asia for
Operations Desert Shield and Desert Storm. In January 1995, he entered
the Graduate School of the University of Texas at Austin on the Army's
Advanced Civil Schooling program. He is currently a promotable Captain
in the United States Army, a member of the Army Acquisition Corps, and
is enroute to an assignment as an instructor at West Point in the
Department of Civil and Mechanical Engineering.

████████████ress: ████████████████████████
                         ████████████████████████

This thesis was typed by the author.